AMERICAN SOCIETY FOR MICROBIOLOGY | Microbiology Spectrum

RESEARCH ARTICLE

Role of *Staphylococcus agnetis* and *Staphylococcus hyicus* in the Pathogenesis of Buffalo Fly Skin Lesions in Cattle

Muhammad Noman Naseem,[a] Conny Turni,[a] Rosalind Gilbert,[a,b] Ali Raza,[a] Rachel Allavena,[c] Michael McGowan,[c] Constantin Constantinoiu,[d] Chian Teng Ong,[a] Ala E. Tabor,[a,e] Peter James[a]

[a]The University of Queensland, Queensland Alliance for Agriculture and Food Innovation, Centre for Animal Science, St. Lucia, Queensland, Australia
[b]Department of Agriculture and Fisheries, EcoSciences Precinct, Dutton Park, Queensland, Australia
[c]The University of Queensland, School of Veterinary Science, Gatton, Queensland, Australia
[d]James Cook University, College of Public Health, Medical & Veterinary Sciences, Townsville, Queensland, Australia
[e]The University of Queensland, School of Chemistry & Molecular Biosciences, St. Lucia, Queensland, Australia

ABSTRACT Buffalo flies (*Haematobia irritans exigua*) are hematophagous ectoparasites of cattle causing production and welfare impacts in northern Australian herds. Skin lesions associated with buffalo fly infestation and *Stephanofilaria* nematode infection are manifested as focal dermatitis or ulcerated areas, most commonly on the medial canthus of the eye, along the lateral and ventral neck, and on the abdomen of cattle. For closely related horn flies (*Haematobia irritans irritans*), *Staphylococcus aureus* has been suggested as a contributing factor in the development of lesions. To investigate the potential role of bacterial infection in the pathogenesis of buffalo fly lesions, swabs were taken from lesions and normal skin, and bacteria were also isolated from surface washings of buffalo flies and surface-sterilized homogenized flies. Bacterial identification was conducted by matrix-assisted laser desorption ionization–time of flight (MALDI-TOF) and strain typing by repetitive sequence-based PCR (rep-PCR) and DNA sequencing to determine species similarity and virulence factors. Of 50 bacterial isolates collected from lesions, 38 were identified as *Staphylococcus agnetis* and 12 as *Staphylococcus hyicus*, whereas four isolates from normal skin were *S. hyicus* and one was *Mammaliicoccus sciuri*. Of the *Staphylococcus* isolates isolated from buffalo flies, five were identified as *S. agnetis* and three as *S. hyicus*. Fifty percent of the buffalo fly isolates had rep-PCR genotypic patterns identical to those of the lesion isolates. Genome sequencing of 16 *S. agnetis* and four *S. hyicus* isolates revealed closely similar virulence factor profiles, with all isolates possessing exfoliative toxin A and C genes. The findings from this study suggest the involvement of *S. agnetis* and *S. hyicus* in buffalo fly lesion pathogenesis. This should be taken into account in the development of effective treatment and control strategies for lesions.

IMPORTANCE Skin lesions in cattle associated with feeding by *Haematobia* fly species are a significant welfare issue in Australia, North and South America, and Europe. The development of these lesions has been attributed to a number of causal factors, but the exact etiology and pathogenesis were unclear. This study characterized *Staphylococcus agnetis* and *Staphylococcus hyicus* strains from cattle skin lesions and in vector flies and demonstrated their role in the pathogenesis of these lesions. These findings will aid the development of targeted and more effective treatment and control strategies for lesions associated with fly infestation in cattle.

KEYWORDS *Staphylococcus agnetis*, *Staphylococcus hyicus*, *Haematobia*, buffalo fly lesions, cattle, exfoliative toxin

Buffalo flies (BFs) (*Haematobia irritans exigua*) are hematophagous ectoparasites, closely related to horn flies (HFs) (*Haematobia irritans irritans*), which feed mainly on cattle and buffaloes (1–3). Buffalo flies occur in the tropical and subtropical parts of

Editor Catherine Ayn Brissette, University of North Dakota

Address correspondence to Peter James, p.james1@uq.edu.au.

The authors declare no conflict of interest.

Received 11 March 2022
Accepted 9 June 2022
Published 11 July 2022

Australia and Asia and other parts of Oceania, while HFs are prevalent in South and North America and Europe (4). In Australia, cattle skin lesions associated with BF feeding are termed BF lesions. These lesions can range from raised, dry, alopecic, hyperkeratotic, or scab-encrusted areas to severe open suppurating wounds occurring mainly near the medial canthus of the eye, neck, and ventral midline (5). Although these lesions are associated with BF feeding, Sutherst et al. reported a low correlation between BF counts and lesion development (6).

An unnamed species of *Stephanofilaria* nematode has been implicated in the development of these lesions (5), but nematodes were detected in only 40% of skin lesions (7). Naseem et al. suggested that *Stephanofilaria* sp. infection might not be essential for BF lesion development as their study found only 10.83% of lesions infected with *Stephanofilaria* sp., with no nematodes found in either lesions or BFs in some regions of Australia despite the frequent occurrence of lesions (8). Horn flies are reported as vectors for *Stephanofilaria stilesi* nematodes, which have also been implicated in the development of skin lesions in cattle in North and South America (1). However, hypersensitivity to HF feeding and the involvement of *Staphylococcus aureus* have also been suggested as contributing causes in the development of these lesions (9, 10). These findings suggest that other factors might be involved in the development of BF lesions.

In the United States, HFs have been identified as vectors of *Staphylococcus aureus* bacteria, which have been isolated from lesions on the teats and udders of dairy cattle (9). Nickerson et al. showed that dairy farms using HF control presented lower rates of *S. aureus* intramammary infection than herds without control (11), and later, Gillespie et al. confirmed that *S. aureus* isolates from HF had DNA fingerprints identical to 95% of *S. aureus* isolates from mammary secretions and streak canal swabs (12). In addition, *S. aureus*, *Staphylococcus saprophyticus*, *Staphylococcus hyicus*, and *Mammaliicoccus sciuri* have been identified in the microbiome of HF (13).

Staphylococcus hyicus has also been isolated from fresh, encrusted, dry, and old healing skin lesions on the back, shoulder, and root of the tail of cattle, and experimental inoculation with *S. hyicus* produced lesions with a similar clinical appearance (14). Hazarika et al. also isolated *S. hyicus* from skin lesions around the eye, forehead, neck, shoulder, hump, and trunk of cattle and reproduced skin lesions in rabbit skin by experimental inoculation with isolated *S. hyicus* (15). *Staphylococcus hyicus* has also been identified as the causative agent of skin lesions in horses and goats and exudative epidermitis (greasy pig disease) in swine (16–19). In addition, *S. hyicus* isolates from exudative epidermitis of pigs were found to produce epidermolytic exfoliative toxins, which damaged the superficial layer of the skin (20, 21). In all of these studies, phenotypic methods were used for the identification and differentiation of staphylococcal species. Adkins et al. (22) developed the first PCR assay to differentiate *S. hyicus* from *S. agnetis*, revealing that the majority of their previously identified *S. hyicus* isolates from cattle were *S. agnetis*. It is likely that previously identified *S. hyicus* from skin lesions of cattle may have also been misidentified.

The foregoing observations led to the hypothesis that bacterial infections could also have a role in the pathogenesis of BF lesions. In this study, we isolated and identified *Staphylococcus* spp. from BFs and BF lesions from different north Australian beef herds, sequenced the genomes of selected *Staphylococcus* isolates, and investigated the presence of virulence factors in various isolates to assess the potential role of bacteria in the development of BF lesions.

RESULTS

Bacterial isolation. Forty-two lesion swabs were collected from 34 cattle, with two swabs from two separate lesions from eight animals. All lesion swabs produced small, round, white, nonhemolytic, Gram-positive *staphylococcus*-like colonies on blood agar. Swabs from active lesions yielded pure cultures, while swabs from partially active lesions produced mixed cultures with dominant growth of *staphylococcus*-like colonies.

All six lesion swabs from herd 1 (H1) produced growth of *Staphylococcus* spp., with four swabs yielding a pure culture. Swabs from normal skin of the H1 heifers did not produce

any bacterial growth resembling that seen with the lesion swabs. Buffalo fly surface rinses from one animal yielded three colonies of *Staphylococcus* spp., while pure cultures of *Staphylococcus* spp. were isolated from homogenized BFs plated from two animals with lesions. All eight lesion swabs from H2 also yielded *Staphylococcus* growth, with pure cultures obtained from six lesions. Three swabs from normal skin of H2 steers (including one from a steer without lesions) produced one to two colonies of *Staphylococcus* spp. with abundant environmental contaminants, whereas one swab from the normal skin of an animal with lesions yielded two colonies of *M. sciuri*. A pure culture of *Staphylococcus* spp. was isolated from homogenized BFs collected from two steers (one with lesions and one without lesions). Twelve swabs from H3 produced *Staphylococcus* colonies, with very heavy growth from four lesion swabs. *Staphylococcus*-like colonies of various sizes were present on seven swabs from H3. Multiple colonies (one representative from each size variant) were purified by subculture. Eight lesion swabs collected from H4 also yielded staphylococcal growth in blood agar, and the bacteria were isolated as pure cultures from three swabs. A normal skin swab from one H4 animal produced only one colony of *Staphylococcus* sp., while BF washings from one animal and homogenized BFs from two animals yielded two *staphylococcus*-like colonies and heavy *staphylococcus*-like growth, respectively. All swabs collected from H1 and H2 in 2021 had *staphylococcus*-like growth, with pure cultures grown from two swabs.

In initial identification by matrix-assisted laser desorption ionization–time of flight (MALDI-TOF), 43 of 44 isolates from 2020 were identified as *S. hyicus*, and one normal skin isolate was identified as *M. sciuri*. Since MALDI-TOF was unable to differentiate *S. hyicus* and *S. agnetis*, identification of these staphylococcal isolates to the species level was inconclusive at this point. The MALDI-TOF technique was not used to identify any isolates from the 2021 sampling from H1, H2, and H4. All the 2020 and 2021 isolates were reidentified by PCR, and no bacterial growth was observed following plating on MacConkey agar.

Strain typing by rep-PCR. Strain typing by repetitive sequence-based PCR (rep-PCR) was completed on all 44 isolates collected in 2020 from lesions, BFs, and unaffected skin which had been identified by MALDI-TOF as described above. From these 44 isolates, 21 different banding patterns (cluster/pattern types 1 to 21) were identified at a 90% similarity cutoff value. Overall, 10 clusters contained a single isolate, five clusters contained two isolates, and the remaining six clusters contained more than two isolates. Thirty-five isolates from the lesions belonged to 17 different clusters, of which six clusters consisted of a single isolate. Five isolates from the BFs were placed in three clusters, with three isolates being in a cluster with a lesion isolate, while two isolates belonged to single isolate clusters. Four isolates from normal skin showed four different strain types, one of which was *M. sciuri*, as distinguished based on a banding pattern different from those of most of the other isolates. Only one isolate from the normal skin had a similar strain pattern, with one lesion isolate from the same animal.

Among the 19 isolates collected in 2021, 15 different patterns were observed (cluster/pattern types 22 to 36), of which 13 were identified only once. Upon comparison, none of the 2021 isolates showed strain similarity with any of the 21 strain types isolated in 2020. The same pattern was observed from normal skin on one animal, one BF, and two lesion isolates from 2021 collections. There were no differences between the strain types of isolates from different herds. The details for the cluster/pattern type of each isolate are provided in Table 1.

Genome assemblies and annotation. To genetically characterize and determine the role of the bacterial isolates associated with lesion development, 21 isolates (one representative from each cluster/pattern type) from the 2020 sampling were selected for whole-genome sequencing and virulence factor analysis (Table 1). In this study, we generated draft *de novo* genome assemblies for 12 representative isolates (8 from lesions, 2 from BFs, and 2 from normal skin) from 2 $\times$ 150-bp paired Illumina reads. For the rest of the 9 representative isolates (8 from lesions and 1 from BFs), we generated complete, finished *de novo* genome assemblies by hybrid assembly approaches using

TABLE 1 Isolation and identification of bacterial isolates in this study

Herd	Animal ID	Yr	Isolate ID	Sample type[a]	Cluster/ pattern (rep-PCR)	PCR/ sequencing identification
H1	C1	2020	BR2785	Eye lesion, R	3	*S. agnetis*
H1	C2	2020	BR2788	Eye lesion, R	5	*S. agnetis*
H1	C3	2020	BR2789	Eye lesion, L	5	*S. agnetis*
H1	C4	2020	BR2786[b]	Eye lesion, L	8	*S. agnetis*
H1	C5	2020	BR2787[b]	Belly lesion	5	*S. agnetis*
H1	C6	2020	BR2795[c]	Belly lesion	6	*S. agnetis*
H1	C7	2021	BR2910	Eye lesion, R	31	*S. agnetis*
H1	C8	2021	BR2906	Eye lesion, R	32	*S. agnetis*
H1	C9	2021	BR2911	Eye lesion, R	33	*S. agnetis*
H1	C10	2021	BR2908	Eye lesion, L	34	*S. agnetis*
H1	C8	2021	BR2909	Shoulder lesion	32	*S. agnetis*
H1	C4	2020	BR2804[c]	Homogenized BFs	3	*S. agnetis*
H1	C3	2020	BR2806	Homogenized BFs	3	*S. agnetis*
H1	C3	2020	BR2807	BF washings	3	*S. agnetis*
H2	C11	2020	BR2832[b]	Eye lesion, L	7	*S. agnetis*
H2	C12	2020	BR2816[c]	Eye lesion, L	13	*S. agnetis*
H2	C13	2020	BR2820[c]	Eye lesion, R	17	*S. hyicus*
H2	C14	2020	BR2823[b]	Eye lesion, R	19	*S. hyicus*
H2	C15	2020	BR2824	Eye lesion, L	19	*S. hyicus*
H2	C15	2020	BR2825	Eye lesion, R	19	*S. hyicus*
H2	C16	2020	BR2829[c]	Eye lesion, R	20	*S. hyicus*
H2	C17	2021	BR2917	Eye lesion, L	35	*S. hyicus*
H2	C18	2021	BR2918	Eye lesion, R	36	*S. hyicus*
H2	C12	2020	BR2815	Dewlap lesion	13	*S. agnetis*
H2	C13	2020	BR2821	Normal skin	17	*S. hyicus*
H2	C19	2020	BR2827	Normal skin	19	*S. hyicus*
H2	C16	2020	BR2831[b]	Normal skin	21	*S. hyicus*
H2	C14	2020	BR2822[b]	Normal skin	18	*M. sciuri*
H2	C16	2020	BR2828[b]	Homogenized BFs	4	*S. agnetis*
H2	C20	2020	BR2814[b]	Homogenized BFs	14	*S. agnetis*
H3	C21	2020	BR2841	Eye lesion, R	1	*S. agnetis*
H3	C21	2020	BR2842	Eye lesion, R	1	*S. agnetis*
H3	C22	2020	BR2846	Eye lesion, R	3	*S. agnetis*
H3	C23	2020	BR2847[c]	Eye lesion, R	1	*S. agnetis*
H3	C23	2020	BR2848	Eye lesion, R	1	*S. agnetis*
H3	C23	2020	BR2849	Eye lesion, L	1	*S. agnetis*
H3	C24	2020	BR2851	Eye lesion, L	1	*S. agnetis*
H3	C24	2020	BR2852	Eye lesion, R	1	*S. agnetis*
H3	C25	2020	BR2845[c]	Eye lesion, L	2	*S. agnetis*
H3	C26	2020	BR2862[b]	Eye lesion, R	9	*S. agnetis*
H3	C26	2020	BR2863	Eye lesion, R	9	*S. agnetis*
H3	C27	2020	BR2858[b]	Eye lesion, L	10	*S. agnetis*
H3	C25	2020	BR2844[b]	Eye lesion, L	11	*S. agnetis*
H3	C26	2020	BR2864[c]	Eye lesion, L	12	*S. agnetis*
H3	C26	2020	BR2865	Eye lesion, L	12	*S. agnetis*
H3	C28	2020	BR2859[b]	Eye lesion, L	15	*S. agnetis*
H3	C28	2020	BR2860	Eye lesion, L	15	*S. agnetis*
H3	C28	2020	BR2861	Eye lesion, L	15	*S. agnetis*
H3	C29	2020	BR2855[c]	Eye lesion, R	16	*S. agnetis*
H3	C27	2020	BR2856	Eye lesion, L	16	*S. agnetis*
H3	C27	2020	BR2857	Eye lesion, L	16	*S. agnetis*
H4	C30	2021	BR2885	Eye lesion, L	22	*S. agnetis*
H4	C31	2021	BR2894	Eye lesion, L	28	*S. agnetis*
H4	C32	2021	BR2886	Eye lesion, R	23	*S. hyicus*
H4	C33	2021	BR2890	Eye lesion, L	25	*S. hyicus*
H4	C35	2021	BR2892	Eye lesion, L	26	*S. hyicus*
H4	C36	2021	BR2893	Eye lesion, R	27	*S. hyicus*
H4	C37	2021	BR2895	Neck lesion	26	*S. hyicus*
H4	C34	2021	BR2888	Belly lesion	24	*S. agnetis*
H4	C34	2021	BR2889	Normal skin	26	*S. hyicus*
H4	C32	2021	BR2899	Homogenized BFs	29	*S. hyicus*
H4	C33	2021	BR2897	Homogenized BFs	30	*S. hyicus*
H4	C33	2021	BR2896	BF washings	26	*S. hyicus*

[a]R, right eye; L, left eye.
[b]Sequenced with Illumina NovaSeq 6000.
[c]Sequenced with both Illumina NovaSeq 6000 and MinION (ONT).

TABLE 2 Details of bacterial genome assembly for isolates sequenced in this study

Isolate ID[a]	Assembly status	Genome size (bp)	No. of contigs	Longest contig length (bp)[b]	No. of:			Accession no.
					CDS	rRNAs	tRNAs	
BR2786_aL	Draft	2,481,539	89	304,262	2,402	5	48	JALGOP000000000
BR2787_aL	Draft	2,482,413	112	304,101	2,403	7	58	JALGOO000000000
BR2795_aL	Complete	2,449,123	1	NA	2,465	19	59	JALGON000000000
BR2832_aL	Draft	2,533,020	90	304,049	2,470	6	55	JALGOM000000000
BR2844_aL	Draft	2,440,290	60	225,370	2,358	6	56	JALGOL000000000
BR2845_aL	Complete	2,437,387	1	NA	2,371	19	60	JALGOK000000000
BR2847_aL	Complete	2,414,453	1	NA	2,423	19	59	JALGOJ000000000
BR2855_aL	Complete	2,481,102	1	NA	2,465	19	60	JALGOI000000000
BR2858_aL	Draft	2,404,324	53	318,300	2,334	3	42	JALGOH000000000
BR2859_aL	Draft	2,472,985	69	194,377	2,402	3	43	JALGOG000000000
BR2862_aL	Draft	2,434,216	76	229,021	2,359	6	46	JALGOF000000000
BR2864_aL	Complete	2,438,730	1	NA	2,373	3	42	JALGOE000000000
BR2816_aL	Complete	2,506,912	1	NA	2,517	19	59	JALGOD000000000
BR2804_aB	Complete	2,462,691	1	NA	2,539	19	60	JALGOC000000000
BR2814_aB	Draft	2,492,807	88	303,910	2,429	4	51	JALGOB000000000
BR2828_aB	Draft	2,485,945	88	181,960	2,426	4	42	JALGOA000000000
BR2820_hL	Complete	2,434,473	1	NA	2,390	19	59	JALGNZ000000000
BR2823_hL	Draft	2,597,767	38	489,936	2,556	4	72	JALGNY000000000
BR2829_hL	Complete	2,452,563	1	NA	2,369	19	62	JALGNX000000000
BR2831_hN	Draft	2,519,724	76	270,422	2,448	4	75	JALGNW000000000
BR2822_sN	Draft	2,784,109	135	251,211	2,760	3	43	JALGNV000000000

[a]The suffixes aL, aB, sN, hL, and hN indicate *S. agnetis* from lesions, *S. agnetis* from buffalo flies, *M. sciuri* from normal skin, *S. hyicus* from lesions, and *S. hyicus* from normal skin, respectively.
[b]NA, not applicable.

Illumina and Oxford Nanopore Technologies (ONT) reads. Assembly details (assembly status, number of contigs, genome size, number of CDS, rRNA, and tRNA) for each isolate sequenced are provided in Table 2. The draft genome assemblies ranged from 38 to 115 contigs, comprising 2.40 to 2.78 Mbp. The hybrid assemblies comprised a single circular contig and range from 2.41 to 2.50 Mbp. The numbers of coding sequences (CDS), rRNAs, and tRNAs varied between isolates and ranged from 2,334 to 2,769, 3 to 19, and 42 to 75, respectively (Table 2).

Pangenome analysis, read mapping, and multilocus sequence analysis. The initial pangenome analysis of all 20 sequenced *Staphylococcus* species isolates, previously identified as *S. hyicus* by MALDI-TOF, indicated that there were 754 core genes (i.e., genes found in 99% to 100% of strains), 3 soft core genes (95% to 99% of strains), 3,429 shell genes (15% to 95% of strains), and 2,024 cloud genes (0% to 15% of strains). The smaller number of core genes and the high number of cloud genes indicates that the 20 sequences of isolates initially identified as *S. hyicus* might actually be different *Staphylococcus* species, rather than strains within a species. A pangenome analysis for all sequenced isolates is presented in Fig. 1.

To confirm the sequence isolate identity, corrected paired Illumina reads from each isolate sequenced were mapped against the genomes of reference strains of *S. hyicus*, *S. agnetis*, *S. chromogenes* and *M. sciuri*. Of the 21 sequenced isolates, 80.5% to 90.32% of paired Illumina reads from 16 isolates were mapped with *S. agnetis*, while $<$30% and $<$10% of the reads from these 16 isolates were mapped with reference genomes of *S. hyicus* and *S. chromogenes*, respectively. From the remaining isolates, 78 to 82% of the reads from four isolates mapped with *S. hyicus*, but $<$30% and $<$10% of the reads from these four isolates mapped with reference genomes of *S. agnetis* and *S. chromogenes*, respectively. The 89.5% reads from the *M. sciuri* isolate obtained from this study, mapped exactly with the reference genome of *M. sciuri*.

The argument for reclassifying 16 of the *Staphylococcus* isolates was further strengthened when a pangenome analysis of these 16 suspected *S. agnetis* isolates resulted in 1,981 core genes, 0 soft core genes, 806 shell genes, and 896 cloud

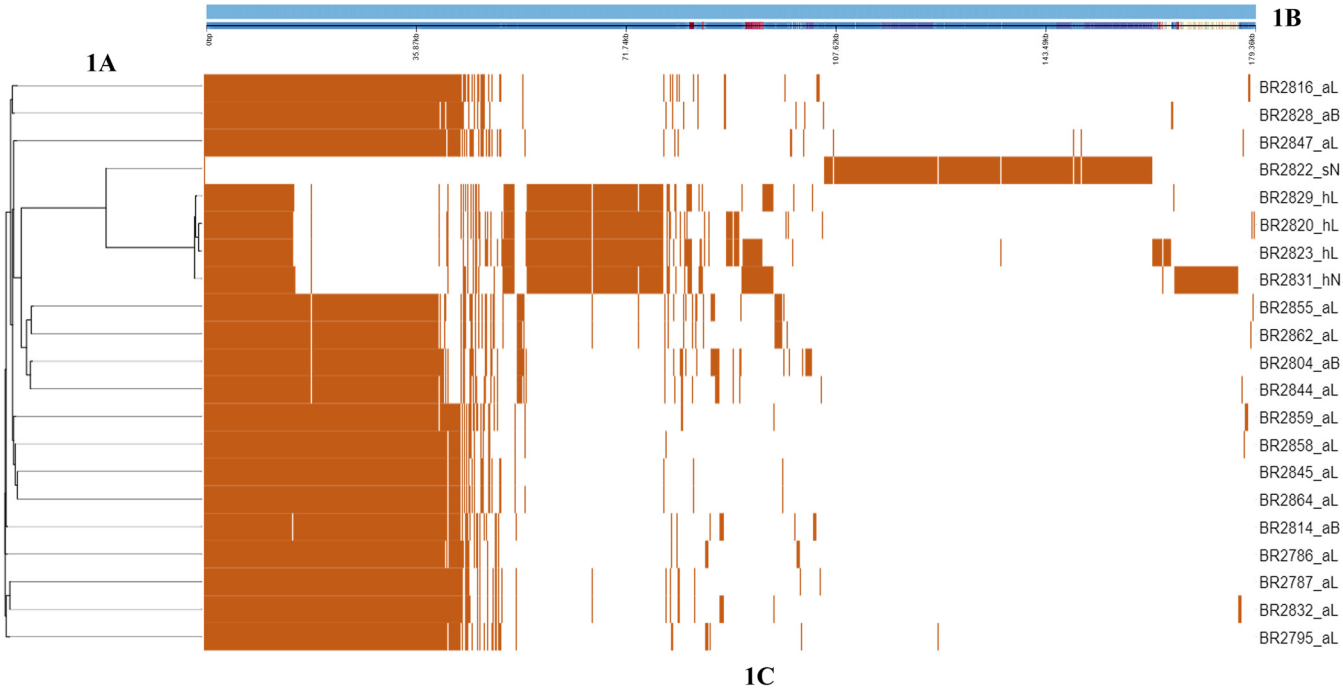

FIG 1 (A) The pangenome analysis indicates a similar and unique gene group among all the sequenced isolates with a core genome phylogenetic tree. (B) Single representative nucleotide sequence inferred for each gene of the pangenome. (C) Presence (orange) or absence (white) of blocks relative to the genes and contigs in the pan-genome. For isolate designations, the suffixes aL, aB, sN, hL, and hN indicate *S. agnetis* from lesions, *S. agnetis* from buffalo flies, *M. sciuri* from normal skin, *S. hyicus* from lesions, and *S. hyicus* from normal skin, respectively.

genes. This finding indicated that these 16 isolates were *S. agnetis*. Pangenome analysis of the four confirmed *S. hyicus* isolates resulted in the identification of 810 core genes, 0 soft core genes, 4,211 shell genes, and 0 cloud genes, indicating more strain variation among these isolates.

The identity of 21 sequenced isolates was confirmed by a multilocus sequence phylogenetic analysis based on four housekeeping genes (*tuf*, *rpoA*, *rpoB*, and *recN*) (Fig. 2). This showed that all 16 suspected *S. agnetis* isolates clustered (97% branch threshold of homology) with the reference strain of *S. agnetis* (DSM23656) and a bovine mastitis isolate of *S. agnetis* (1379). This confirmed that these 16 isolates belonged to the species *S. agnetis*. Four additional *S. hyicus* isolates clustered strongly (99% branch threshold of homology) with the reference strain of *S. hyicus* (NCTC10350), while one *M. sciuri* isolate from the current study clustered with the reference strain of *M. sciuri* (NCTC12103) (Fig. 2).

Staphylococcal VF identification. We identified 13 genes that belonged to eight virulence factors (VF) of the adherence category, including those encoding autolysin (*atl*), clumping factors (*clfA* and *clfB*), collagen adhesion (*cna*), fibrinogen binding proteins (*efb*), fibronectin-binding proteins (*fnbA* and *fnbB*), intracellular adhesin (*icaA*, *icaB*, and *icaC*), Ser-Asp-rich fibrinogen binding proteins (*sdrD* and *sdrF*), and staphylococcal protein A (*spa*). The distribution and percentage similarities for the staphylococcal VF genes identified are provided in Fig. 3. The distribution of the VF varied between the species isolated as well as between strains within species. The autolysin gene (*atl*) was the only gene identified in all the *Staphylococcus* isolates for which genome sequencing was undertaken. The VF genes responsible for adherence identified in the genome sequences of all the *S. agnetis* isolates were almost the same, except that *clfA*, *clfB*, *sdrD*, and *sdrF* were present in 87.5%, 93.75%, 75%, and 62.5% of the isolates, respectively. Similarly, VF genes responsible for adherence identified in the genome sequences of the *S. hyicus* isolates were also the same, except that *clfA*, *efb*, and *sdrD* were absent in the single isolate obtained from a normal skin sample. The staphylococcal protein A gene (*spa*) was found only in the *S. hyicus* isolates, whereas *clfA*, *clfB*, *cna*, *efb*, *fnbA*, *fnbB*, *sdrD*, and *sdrF* were not identified in the *M. sciuri* isolate, which instead contained *icaA*, *icaB*, and *icaC*.

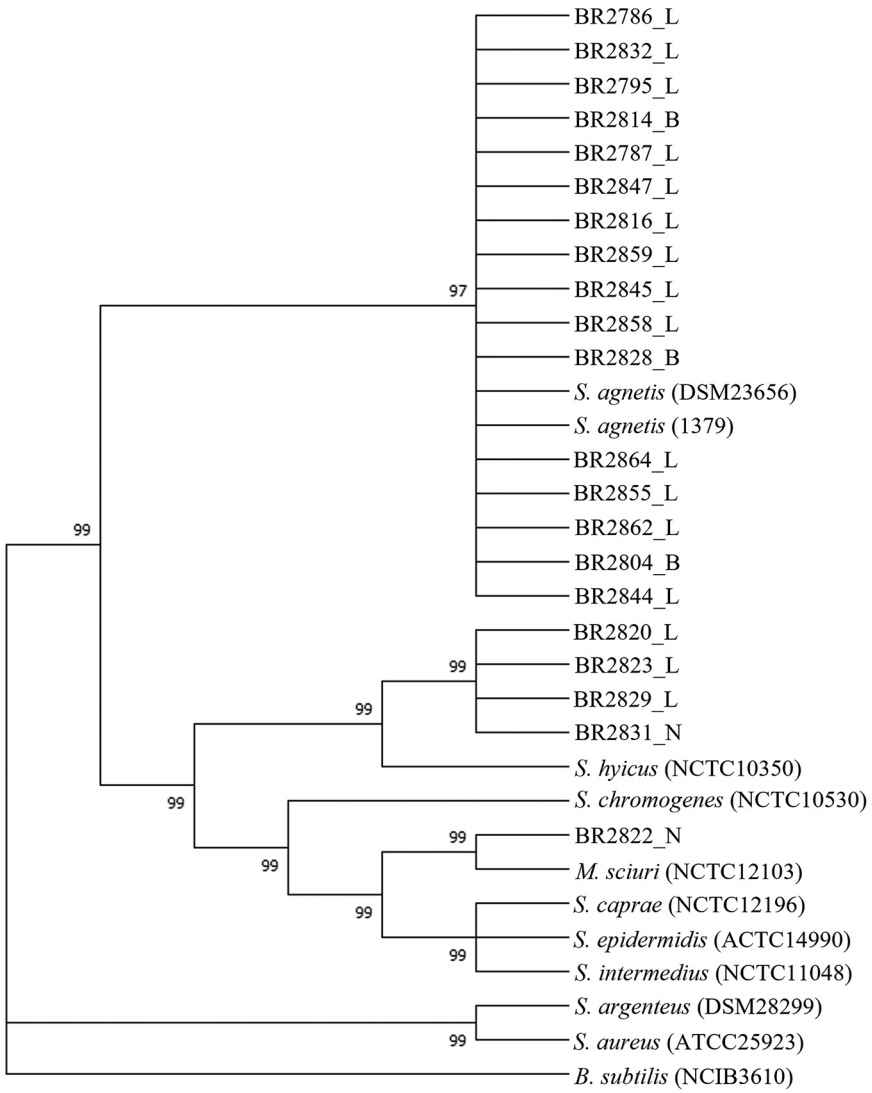

FIG 2 Maximum-likelihood multilocus tree built from concatenated nucleotide sequence alignment of four housekeeping genes (*tuf*, *rpoA*, *rpoB*, and *recN*) of all the isolates and other closely related *Staphylococcus* spp. Bootstrap branch support (based on likelihood analysis) is shown. For isolate designations, the suffixes L, B, and N indicate "from lesion," "from buffalo flies," and "from normal skin," respectively.

Among the exoenzymes examined, we identified nine VF, including aureolysin (*aur*), adenosine synthase A (*adsA*), cysteine protease (*sspB*), lipases (*geh* and *lip*), serine V8 protease (*sspA*), staphylokinase (*sak*), thermonuclease (*nuc*) and von Willebrand factor-binding protein (*vWbp*). Of these, *aur* and *nuc* were the only genes identified in all the sequenced *Staphylococcus* isolates. Most of the exoenzyme genes identified within the *S. agnetis* isolate were similar, except for the gene *geh*, which was found in 68.75% of the isolates. Similarly, VF genes for exoenzymes were mainly similar in the *S. hyicus* isolates, except for the genes *geh*, *lip*, and *sak*, which were present in 75%, 75%, and 50% of the isolates, respectively. The gene *sspA* was present in only the *M. sciuri* isolate.

The VF category involved in host immune evasion consists of genes for capsule formation (*capA*, *capB*, *capC*, *capD*, *capE*, *capF*, *capG*, *capH*, *capI*, *capJ*, *capK*, *capL*, *capM*, *capN*, *capO*, and *capP*) and the staphylococcal binder of immunoglobulin (*sbi*). The gene *sbi* was identified in the genome sequences of all isolates except the *M. sciuri* isolate. All the capsule-forming genes classified in the host immune evasion VF category were identified in the genome sequence of all the *S. agnetis* isolates characterized. The gene *capJ*, however,

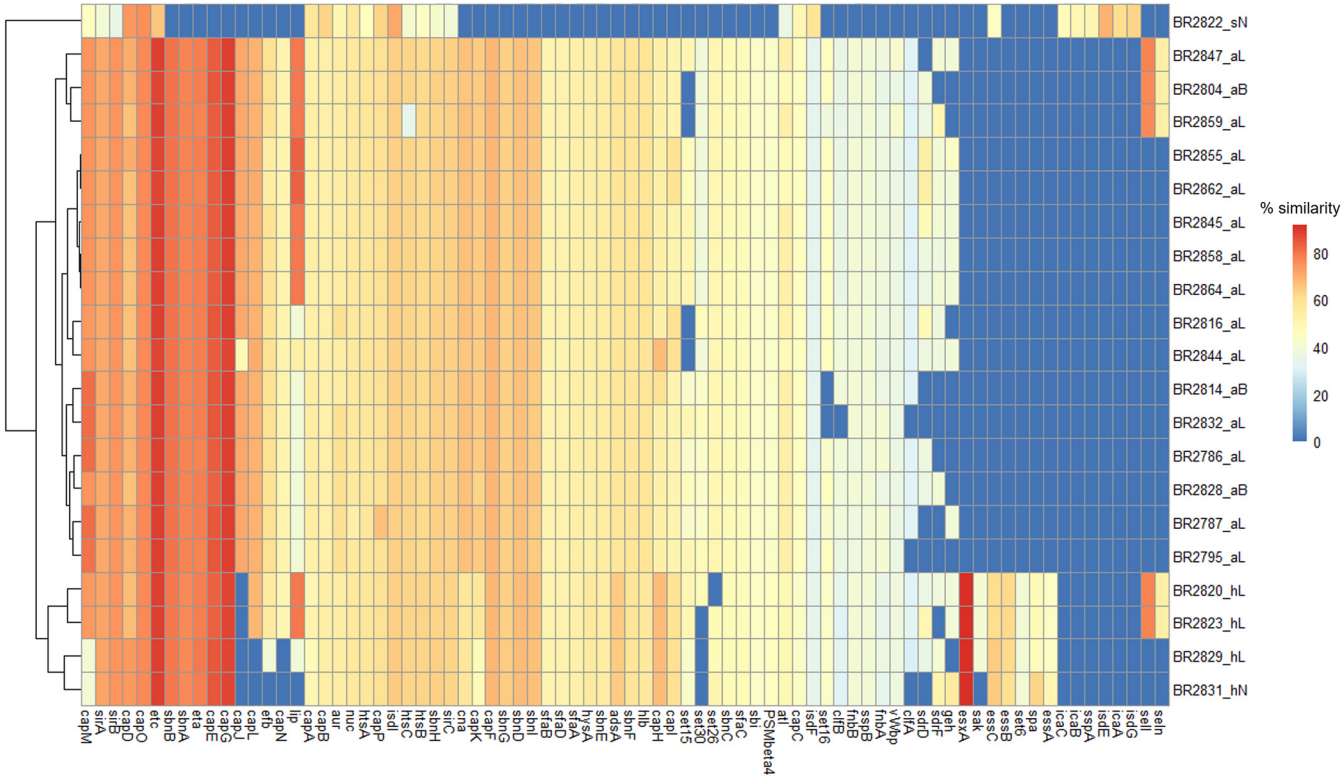

FIG 3 Heat map showing distribution and amino acid sequence similarities of different VF genes in the 21 sequenced isolates from 2020 with the VF sequences of *Staphylococcus* spp. in the databases. The dendrogram indicates clustering of isolates based on the presence or absence and percentage similarities of different VF. The genes for adherence category include *atl*, *clfA*, *clfB*, *can*, *efb*, *fnbA*, *fnbB*, *icaA*, *icaB*, *icaC*, *sdrD*, *sdrF*, and *spa*. The genes *aur*, *adsA*, *sspB*, *geh*, *lip*, *sspA*, *sak*, *nuc*, and *nuc* belong to exoenzyme-type VF. The genes responsible for host immune evasion include capsule-forming genes (*capA*, *capB*, *capC*, *capD*, *capE*, *capF*, *capG*, *capH*, *capI*, *capJ*, *capK*, *capL*, *capM*, *capN*, *capO*, and *capP*) and staphylococcal binder of immunoglobulin (*sbi*). The genes responsible for iron uptake and metabolism include *isdE*, *isdF*, *isdG*, *isdI*, *htsA*, *htsB*, *htsC*, *sfaA*, *sfaB*, *sfaC*, *sfaD*, *sirA*, *sirB*, *sirC*, *sbnA*, *sbnB*, *sbnC*, *sbnD*, *sbnE*, *sbnF*, *sbnG*, *sbnH*, and *sbnI*. The genes involved in the type VII secretion system include *essA*, *essB*, *essC*, and *essD*. The gene *seln* and *sell* encode exotoxins, while *set6*, *set15*, *set16*, *set26*, and *set30* are for enterotoxin. The exfoliative toxins A and C are encoded by *eta* and *etc,* respectively. The genes *hlb* and *PSMβ4* are hemolysin and phenol-soluble-modulin genes, respectively. For isolate designations, the suffixes aL, aB, sN, hL, and hN indicate *S. agnetis* from lesions, *S. agnetis* from buffalo flies, *M. sciuri* from normal skin, *S. hyicus* from lesions, and *S. hyicus* from normal skin, respectively.

was absent in all *S. hyicus* isolates, while *capL* and *capN* were not found in 50% of the genome sequences for this species. In addition, the *M. sciuri* isolate had only *capA*, *capB*, *capC*, *capD*, *capM*, *capO*, and *capP* genes for capsule formation within the whole-genome sequence.

For iron uptake and metabolism VF categories, 23 genes were identified, including four iron-regulated surface determinant genes (*isdE*, *isdF*, *isdG*, and *isdI*), seven ATP-binding cassette (ABC) transporter (siderophore receptor) genes (*htsA*, *htsB*, *htsC*, *sfaA*, *sfaB*, *sfaC*, and *sfaD*), three staphyloferrin A synthesis related genes (*sirA*, *sirB*, and *sirC*), and nine staphyloferrin B synthesis related genes (*sbnA*, *sbnB*, *sbnC*, *sbnD*, *sbnE*, *sbnF*, *sbnG*, *sbnH*, and *sbnI*) (Fig. 3). All of the genes responsible for iron uptake and metabolism were identified in all *S. agnetis* and *S. hyicus* isolates except *isdE* and *isdG*, which were identified only in *M. sciuri*. The genes *sbnA*, *sbnB*, *sbnC*, *sbnD*, *sbnE*, *sbnF*, *sbnG*, *sbnI*, *sfaA*, *sfaB*, *sfaC*, and *sfaD* were not identified in *M. sciuri*.

The four genes for the type VII secretion system (*essA*, *essB*, *essC*, and *essD*) were identified in all *S. hyicus* isolates, while *M. sciuri* had only one gene (*essC*). No type VII secretion system gene was found in any of the *S. agnetis* isolates. The beta-hemolysin gene (*hlb*) was identified in all *S. agnetis* and *S. hyicus* isolates but absent in *M. sciuri*. The genes for enterotoxin (*sell* and *seln*) were identified in 50% of *S. hyicus* and 18.75% *S. agnetis* isolates but absent in *M. sciuri*. All the isolates of *S. agnetis* and *S. hyicus* were found to have exfoliative toxin A and C genes (*eta* and *etc*), while the *M. sciuri* isolate had only the *etc* gene. The genes for exotoxin (*set26* and *set30*) were identified in all the *S. agnetis* isolates, while the genes *set15* and *set16* were present in only 81.25%

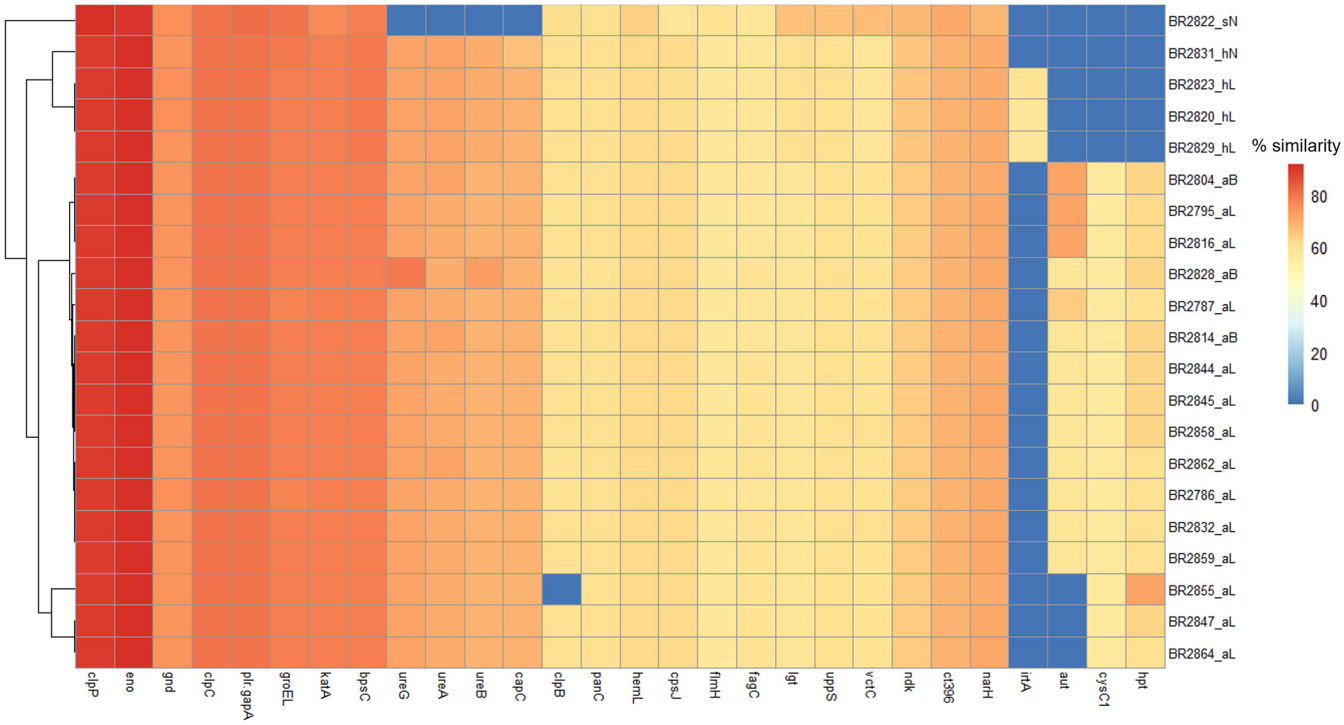

FIG 4 Heat map showing distribution and amino acid sequence similarities of different VF genes in all sequenced isolates with the VF sequences of nonstaphylococcal species in the databases. The dendrogram indicates clustering of isolates based on the presence or absence and percentage similarities of different VF. This includes genes for the enzyme VF category (*ureA*, *ureB*, *ureG*, *gnd*, *katA*, *cysC1*, *clpP*, *capC*, *groEL*, *clpC*, f*lmH*, *hemL*, *aut*, *narH*, *ndk*, *panC*, *bpsC*, *uppS*, *eno*, and *lgt*) and additional genes for iron uptake and metabolism (*fagC*, *vctC*, *cpsJ*, and *iraT*). The genes *plr/gapA*, *hpt*, and *lplA* encode putative proteins. For isolate designations, the suffixes aL, aB, sN, hL, and hN indicate *S. agnetis* from lesions, *S. agnetis* from buffalo flies, *M. sciuri* from normal skin, *S. hyicus* from lesions, and *S. hyicus* from normal skin, respectively.

and 87.5% of the isolates, respectively. All *S. hyicus* isolates carried *set6*, *set15*, and *set16* genes for exotoxins, while *set26* and *set30* were found in 75% and 25% of the isolates. The gene for phenol-soluble modulins (*PSMβ4*) was identified in all *S. agnetis* and *S. hyicus* isolate, but no exotoxin or phenol-soluble-modulin genes were observed in *M. sciuri*.

Nonstaphylococcal VF identification. We also identified some VF in our isolates that had ≥50% amino acid homology with VF of nonstaphylococcal species in the VF core data set (VFCD) (Fig. 4). Among these, 22 genes of the VF enzyme category were detected, including those encoding urease (*ureA*, *ureB*, and *ureG*), 6-phosphogluconate dehydrogenase (*gnd*), catalase (*katA*), adenylylsulfate kinase (*cysC1*), ATP-dependent Clp protease proteolytic subunit (*clpP*), capsule biosynthesis protein (*capC*), chaperonin (*groEL*), endopeptidase Clp ATP-binding chain (*clpC*), flagellum-related 3-oxoacyl-ACP (acyl carrier protein) reductase (*flmH*), glutamate-1-semialdehyde-2,1-aminomutase (*hemL*), molecular chaperone (*ct396*), autolysin (*aut*), nitrate reductase (*narH*), nucleoside diphosphate kinase (*ndk*), pantoate–beta-alanine ligase (*panC*), UTP–glucose-1-phosphate uridylyltransferase (*bpsC*), undecaprenyl diphosphate synthase (*uppS*), phosphopyruvate hydratase (*eno*), prolipoprotein diacylglyceryl transferase (*lgt*), and protein disaggregation chaperone (*clpB*). All isolates had almost all the above-mentioned VF genes except the *aut* gene, which was absent in three *S. agnetis*, all *S. hyicus*, and *M. sciuri* isolates. The gene *cysC1* was also absent in all *S. hyicus* and *M. sciuri* isolates. All isolates had three additional genes for iron uptake and metabolism, including *fagC*, *vctC*, and *cpsJ*, whereas the fourth gene, *iraT*, was found only in three *S. hyicus* isolates from lesions. Three genes for putative proteins (*plr/gapA*, *hpt*, and *lplA*) were identified in all *S. agnetis* isolates, while *S. hyicus* and *M. sciuri* exhibited only *plr/gapA* and *lplA*.

Exfoliative toxin analysis. Exfoliative toxin A (*eta*) identified from all *S. agnetis* isolates had 89.21% to 89.54% and 77.77% to 78.10% amino acid homology with *exhA* from *S. hyicus* and *eta* from different strains of *S. aureus*, respectively. The *eta* gene from all *S. hyicus* isolates had 94.12% to 95.08% and 78.75% to 79.73% homology with

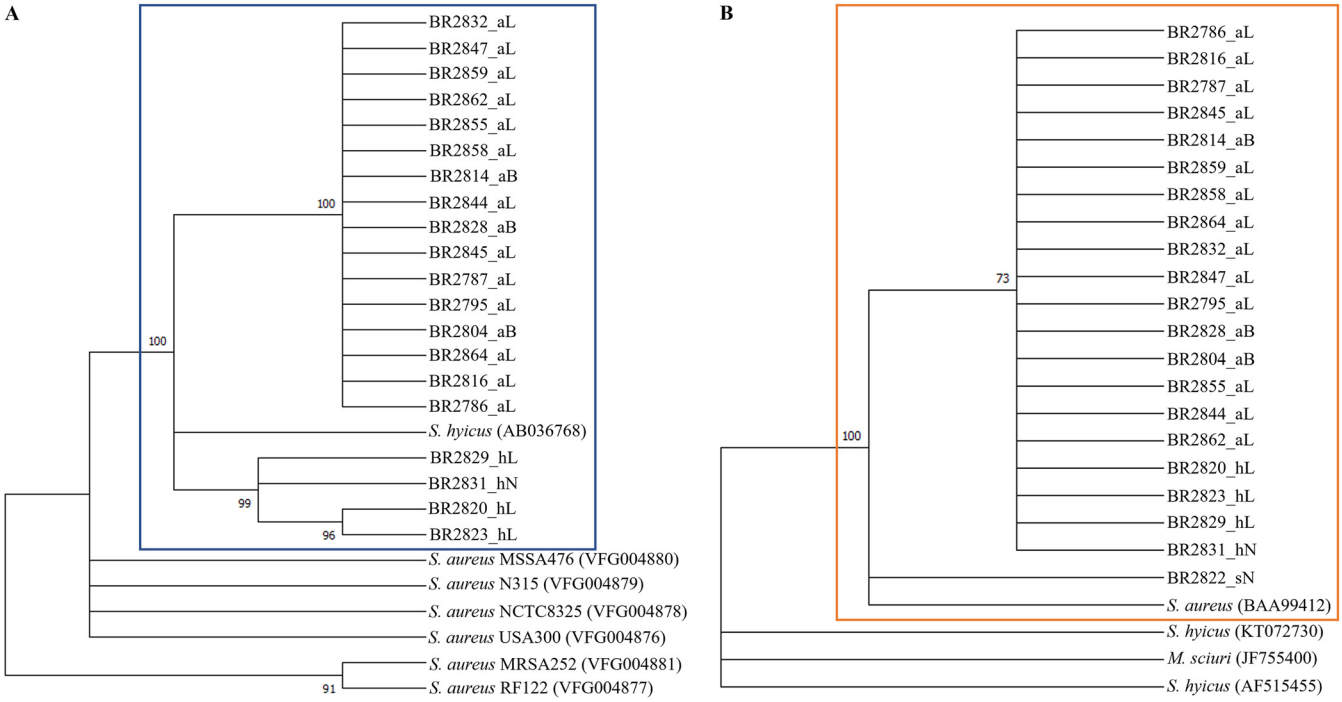

FIG 5 Maximum-likelihood trees built from amino acid sequences of *eta* (A) and *etc* gene (B) from all the sequenced isolates and other closely related staphylococcal species. Bootstrap branch support (based on likelihood analysis) is shown. For isolate designations, the suffixes aL, aB, sN, hL, and hN indicate *S. agnetis* from lesions, *S. agnetis* from buffalo flies, *M. sciuri* from normal skin, *S. hyicus* from lesions, and *S. hyicus* from normal skin, respectively.

exhA from *S. hyicus* and *eta* from different strains of *S. aureus*, respectively. The *eta* gene was not identified in the *M. sciuri* isolate from normal skin.

Evolutionary tree analysis for the *eta* gene showed that all the *eta* sequences from the current study occurred in the same clade as *S. hyicus exhA*, but on different branches (Fig. 5A). Exfoliative toxin C (*etc*) identified from all the isolates had 87.09% to 87.61% amino acid homology with *etc* from *S. aureus*. The *etc* gene from all the isolates had <1% similarity with *S. hyicus* and *M. sciuri*. Evolutionary tree analysis of *etc* gene showed all the *etc* sequences from the current study occurred in the same clade as *S. aureus*, but on different branches (Fig. 5B).

PCR based identification. As MALDI-TOF was unable to differentiate *S. agnetis* from *S. hyicus*, an *aroD* gene-based species-specific PCR amplifying 295 bp for *S. agnetis* and 425 bp for *S. hyicus* was used for reidentification of all isolates. In initial identification by MALDI-TOF, 43 isolates from 2020 were identified as *S. hyicus*, and one normal skin isolate was identified as *M. sciuri*. However, reidentification by *aroD* gene-based PCR identified 35/43 isolates as *S. agnetis* and only 8/43 as *S. hyicus*. From 2021, 11/19 isolates were identified as *S. hyicus* and 8/19 as *S. agnetis*. All the lesion and BF isolates collected from H1 in 2020 and 2021 were identified as *S. agnetis*. From H2, seven lesions and three normal skin isolates were identified as *S. hyicus*, while three lesion and two BF isolates were identified as *S. agnetis*. Two lesion isolates from the year 2021 were also identified as *S. hyicus*. All 20 lesion isolates from H3 were confirmed as *S. agnetis* with species-specific PCR. From H4, five lesion isolates, three BF isolates (two from homogenized BFs and one from washings) and one normal-skin isolate were identified as *S. hyicus*, whereas three lesion isolates were confirmed as *S. agnetis*. The details of isolation, source, and identification of bacterial isolates are provided in Table 1.

DISCUSSION

In the past, the development of *Haematobia*-associated lesions has generally been attributed to the effects of infection with *Stephanofilaria* spp. nematodes transmitted by BFs and HFs, but in a number of studies, the failure to find nematodes in all lesions

has suggested that other causal factors, including bacteria, may also be involved (10, 12). In this study, we identified *S. agnetis* and *S. hyicus* from BFs and BF lesions from different north Australian beef herds using whole-genome sequencing and conducted a subsequent comprehensive VF identification, which indicated a potential role of these bacterial species in lesion pathogenesis.

All BF lesions sampled in this study were found to be infected with either *S. agnetis* or *S. hyicus*, and the bacteria were isolated in pure cultures from unscabbed lesions. *Staphylococcus hyicus* has been reported as a causative agent of skin lesions and intramammary infection in cattle (12, 14, 23) and exudative epidermitis in pigs (19). Devriese and Derycke suggested that *S. hyicus* skin infection in cattle occurred secondary to parasitic infestation (14) but Hazarika et al. reproduced the skin lesions in rabbits by experimental inoculation of *S. hyicus* isolated from cattle skin lesions (15). However, it is necessary to clarify here that all of these studies reporting *S. hyicus* as the cause of cattle skin lesions and intramammary infection used phenotypic methods for species-level identification of isolates. As these methods were not able to differentiate between *S. hyicus* and *S. agnetis*, there is the possibility that some or all of the *S. hyicus* isolates reported in these studies are in fact *S. agnetis*. Al-Rubaye et al. indicated the potential of *S. agnetis* to cause skin lesions following the identification of exfoliative toxin genes similar to *S. hyicus* isolates of swine origin and *S. aureus* of the scalded-skin syndrome in humans (24). Both *S. agnetis* and *S. hyicus* have been isolated as causative agents of bovine mastitis and intramammary infections (12, 22, 25).

We isolated *S. agnetis* in pure culture from surface-sterilized homogenized BFs from four cattle, and a single colony of *S. agnetis* was also isolated from BF exocuticle washings from one animal. Similarly, *S. hyicus* were isolated in pure cultures from BFs from two animals with lesions, whereas one BF washing sample yielded two colonies of *S. hyicus*. Horn flies have also been reported to vector *S. aureus* and transmit bacteria into the teat skin, resulting in the development of abscesses and lesions (9, 11). Anderson et al. isolated *S. aureus* from 55.8% of the HFs collected from three herds with *S. aureus* intramammary infection (26), and Owens et al. found that *S. aureus* can remain active in infected HF without a significant change in the bacterial count for up to 4 days (10). In a 16S rRNA gene-based pyrosequencing microbiome study of HFs, Palavesam et al. identified *S. hyicus* in adult male HFs and HF eggs (13). This 2012 study (13) did not identify any *S. agnetis* in HFs, although this could be because *S. agnetis* was first described as a separate species from *S. hyicus* in 2012 (25).

The 43 *S. agnetis* isolates in our study included 23 different strain types, and the 19 *S. hyicus* isolates were of 12 different strain types. Four strains of *S. agnetis* were isolated from multiple animals, and one of these strains was isolated from lesion samples from two separate herds. Two strains of *S. hyicus* were also identified from BF lesions from multiple animals. Hazarika et al. collected 47 *S. hyicus* isolates from cattle skin lesions which were separated into 10 different strains (15). However, that study used biochemical characterization for strain typing, which was later found to be less efficient than modern methods. Wegener et al. also reported that the pigs with exudative epidermitis were infected with multiple strains of *S. hyicus* (19). Similarly, 42 *S. agnetis* isolates from a mastitis study of a dairy herd showed 23 different banding patterns with pulsed-field gel electrophoresis (PFGE) strain typing (22). Isolation of multiple strains of *S. agnetis* and *S. hyicus* from BF lesions, in combination with previous reports (15, 19, 22) of multiple strain involvement of these species in skin and intramammary infections, suggests that there might be multiple strains of these two species involved in the pathogenesis of BF lesions.

The genotypic patterns of 75% *S. agnetis* isolates (three of 4 isolates) from BFs collected from animals with lesions were identical to those of lesion isolates from two herds, whereas of three *S. hyicus* isolates from BFs, only one (33.33%) showed similarity with two lesion isolates. In a study of mastitis in three herds, Anderson et al. identified eight different genotypic patterns from 244 isolates of *S. aureus* from teats, milk/colostrum, and HFs (26). Of the *S. aureus* isolates from HFs, 82.7% belonged to a single

genotypic group and 51.6% had a genotypic pattern identical to that of the mastitis isolates. Similarly, Gillespie et al. noted that the *S. aureus* isolates from HFs had genotypic patterns similar to those of 95% of *S. aureus* isolates from udder/teat infections in heifers (12), whereas in our study, 50% of BF isolates had genotypic patterns identical to those of the BF lesion isolates. None of the *S. hyicus* isolates from the normal skin had a genotypic pattern similar to that of the lesion isolates from the respective animals except in one instance, and no *S. agnetis* organisms were isolated from the normal skin samples in our study. The isolation of pure cultures of *S. agnetis* and *S. hyicus* from the surface-sterilized homogenized BFs that were similar to lesion isolates suggests that BFs might play an important role in the transmission of these bacteria.

The inability of MALDI-TOF to differentiate between *S. hyicus* and *S. agnetis* species in our study has also been noted previously (27, 28). In our study, this was due to the lack of *S. agnetis* in the MALDI-TOF database used, which meant that a lower percentage of isolates were correctly identified despite a MALDI-TOF score of $\geq$2.0 when this species was not in the database. MALDI-TOF reference libraries are based on 16S gene sequencing, which evaluates proteins and might not be useful for differentiating these species, as 16S rRNA gene sequences of *S. agnetis* isolates showed 99.87 to 99.92% similarity with *S. hyicus* NCTC10350, higher than the recommended cutoff value of 98.7% similarity for differentiating species (29). Taponen et al. also reported 99.7% similarity of 16S rRNA gene sequences between *S. agnetis* isolates and *S. hyicus* ATCC 11249 (25). The complete sequencing of the β subunit of the RNA polymerase (*rpoB*) gene and the elongation factor Tu (*tuf*) gene have been used previously to differentiate *S. hyicus* and *S. agnetis* at significantly higher similarity cutoff values ($\geq$97% and $\geq$98%, respectively) (22, 30). However, from a cross-species gene similarity comparison, we determined that the DNA repair protein gene (*recN*) of *S. agnetis* isolates has 99.34 to 99.76% and 82.32 to 82.44% similarity with *S. agnetis* DSM23656 and *S. hyicus* NCTC10350, respectively, while *recN* gene of *S. hyicus* isolates has 98.75 to 99.10% and 82.14 to 82.44% similarity with *S. hyicus* NCTC10350 and *S. agnetis* DSM23656, respectively. These apparent differences in the *recN* gene sequence similarities of these two species indicate that the *recN* gene can also be used as a potential marker to differentiate these two species.

The 78 different virulence factor genes identified in sequenced isolates in this study are known virulence factors from the genus *Staphylococcus*, and 28 genes had been identified in bacterial species other than *Staphylococcus*. The genes for adherence are similar in both *S. agnetis* and *S. hyicus* isolates, except for the staphylococcal protein A gene (*spa*), which was present only in *S. hyicus* in this study. This finding was consistent with the work of Naushad et al., who reported *spa* genes in all three bovine mastitis *S. hyicus* isolates but not in 13 *S. agnetis* isolates (31). The presence of clumping factor B gene (*clfB*) in all our *S. agnetis* and *S. hyicus* isolates was the only difference between the adherence genes identified in this study and those from the bovine mastitis study of Naushad et al., where only 15% of bovine mastitis *S. agnetis* isolates had this gene (31). The intracellular adhesion genes and biofilm-producing genes (*icaA*, *icaB*, and *icaC*) were identified only in the *M. sciuri* isolate in our study, which is also consistent with the results of previous studies (31, 32).

After adherence to the host surface, bacterial pathogens produce different enzymes which help neutralize the host immune response and promote tissue degradation (33). Our study identified 10 different exoenzyme genes potentially involved in host immune system neutralization, and most of them were common to *S. hyicus* and *S. agnetis* isolated in the current study. The exoenzyme gene profile of isolates from our study was very similar to those previously reported from bovine mastitis isolates of these species (31, 34), except that we identified the gene for lipase enzyme (*geh*) in 11 *S. agnetis* and three *S. hyicus* isolates. Our study also identified three genes responsible for urease activity (*ureA*, *ureB*, and *ureG*) in all isolates except *M. sciuri*, and this is in line with the study by Åvall-Jääskeläinen et al. (34).

Pathogenic bacteria also use encapsulation to evade the host immune system, and staphylococci are well equipped with encapsulation genes, enabling their protection

against phagocytosis and enhancing persistence of infection (35, 36). The *S. agnetis* isolates from our study had all of the previously identified encapsulation genes (*capA* to *capP*), except that the *capJ* gene was absent in all isolates and *capL* and *capN* were absent in 50% of the *S. hyicus* isolates. Similarly, Naushad et al. reported the absence of *capN* gene in all isolates of *S. agnetis* and *S. hyicus*, and *capJ* in *S. hyicus* isolates (31). In addition, Åvall-Jääskeläinen et al. did not find *capH-capK* genes in *S. agnetis* isolates from bovine mastitis in Finland (34).

Bacterial pathogens require iron for replication and to maintain infection, and pathogenic bacteria have various iron acquisition mechanisms (37–39). The profile of iron uptake genes for *S. agnetis* and *S. hyicus* isolates from our study was similar to that in previous reports (31, 34), with four type VII secretion system (T7SS) genes in all *S. hyicus* isolates, but none of the *S. agnetis* isolates had these genes, which was the only virulence factor difference we observed between these two species. The T7SS genes encode a protein secretion pathway, considered important for the virulence of Gram-positive bacteria (40, 41). This finding is similar to that of Åvall-Jääskeläinen et al., who also found lack of T7SS genes in their *S. agnetis* isolates (34). In contrast, Naushad et al. reported six different T7SS genes in 31% and 67% of the *S. agnetis* and *S. hyicus* isolates, respectively (31). Our study also identified the beta hemolysin gene (*hlb*) in all sequenced isolates except *M. sciuri*, which supports the findings of Åvall-Jääskeläinen et al. (34) and Naushad et al. (31).

Identification of exfoliative toxin A (*eta*) and C (*etc*) genes from *S. agnetis* and *S. hyicus* in this study was a major finding in relation to skin lesion development. These toxins are also known as epidermolytic toxins and are serine proteases, able to digest skin desmoglein-1, resulting in the deterioration of desmosomal cell adhesions and epidermal damage (42). The presence of the *eta* gene in *S. agnetis* and *S. hyicus* isolates is in accordance with previous mastitis isolate studies (24, 31, 34), but none of these studies found the *etc* gene in their isolates. Our study also identified the *etc* gene in *M. sciuri* from normal skin, which is contrary to findings of Naushad et al. (31). The close amino acid homology of exfoliative toxins A and C from this study with exfoliative toxins A and C from *S. hyicus* isolated from exudative epidermitis of pigs and *S. aureus* from skin infections in horses indicates that these toxins might play an important role in the epidermal damage in BF lesions. This suggestion is further strengthened by the observations from histological studies of BF lesions, which indicated epidermal damage in all bacterially infected lesions (our unpublished observation). Our study also indicated similarity between the VF profiles of BFs and BF lesion isolates, which further suggests that the BF isolates where the genotype is not similar to that of the lesion isolate are equally pathogenic and may be involved in lesion pathogenesis when transmitted during BF feeding. The close similarity between the VF profiles of *S. agnetis* and *S. hyicus* indicate that both of these species could potentially be involved in the pathogenesis of BF lesions.

Conclusion. The findings from this study indicate that the bacteria *S. agnetis* and *S. hyicus*, vectored by BFs, are likely to be significant factors in the pathogenesis of BF lesions. This suggests that the role of bacteria should be a consideration in the development of optimal treatment and control strategies for BF lesions.

MATERIALS AND METHODS

Sample collection. Samples were collected from cattle (n = 34) with ulcerated to partially scabbed BF lesions from four different herds. Lesions around the eye and on the shoulder, dewlap, and belly of cattle were swabbed using Amies agar gel transport swabs (Copan, Murrieta, CA, USA). Multiple lesion swabs were collected if the animal had more than one lesion. The cattle sampled included five Brahman heifers from herd 1 (H1) and six Brangus steers from H2, kept at the University of Queensland Pinjarra Hills Research Precinct (−27.53, 152.91) in spatially separated paddocks sampled in May 2020. Eight Brahman heifers from a commercial cattle property in north Queensland (H3) (−20.50, 146.0) were sampled in August 2020, and eight Droughtmaster cattle kept at Darbalara farm (−27.59, 152.38) (H4) were sampled in January 2021. One swab was also collected from visually normal skin from each animal (at least 15 cm away from lesions). Lesion swabs from five heifers from H1 and two steers from H2 were sampled again in August and September 2021, respectively, and skin swabs were also collected from

15 cm down the medial canthus from three steers without any lesions from H2. This study was approved by the University of Queensland Animal Ethics committee (approval no. 2021/AE000054).

Buffalo flies were also collected from the back of each swabbed animal with lesions in H1, H2, and H4 and the three steers without lesions from H2 using an insect collection net. The insect net was disinfected with 80% ethanol between collections, and BFs from each collection were transferred to a sterile plastic zip bag, labeled with the animal ID, and transported to the laboratory on ice.

Bacterial isolation. Each swab was used to streak 5% (vol/vol) sheep blood agar and MacConkey agar within 24 h of collection. Buffalo flies (n = 110) were streaked following the method described previously (43). Briefly, five BFs from each animal were washed three times by dipping into 250 μL of sterile normal saline, and the saline washing solution from each group was streaked onto blood agar and MacConkey agar. After washing, the flies were surface disinfected by immersion in 10% sodium hypochlorite (NaClO) followed by 70% ethanol for at least 10 min each. Flies were then rinsed in normal saline, air dried, homogenized in 100 μL of sterile normal saline, and plated on blood agar and MacConkey agar plates. Plates were incubated at 37°C for 24 h. Bacterial colonies were distinguished as Gram-positive or negative by the potassium hydroxide (KOH) test (44).

Species identification by MALDI-TOF. Pure cultures of all isolates (n = 44) from the 2020 sampling were submitted to the Biosecurity Queensland Veterinary Laboratories (Department of Agriculture and Fisheries, Coopers Plains, Queensland, Australia; −27.55, 153.04) for initial species identification by MALDI-TOF mass spectrometry (MALDI-TOF MS) (manufactured by Bruker Daltonics, Germany). A MALDI-TOF score of ≥2.0 was set as the cutoff point for species identification.

DNA extraction. DNA was extracted using the Qiagen DNeasy blood and tissue extraction kit (Qiagen Pty. Ltd., Hilden, Germany) according to the manufacturer's protocol. Briefly, extraction involved suspending a loop full of the bacterial isolate from a fresh overnight blood agar culture into lysis buffer. The suspension was incubated for 1.5 h at 56°C. The remainder of the protocol was as recommended by the manufacturer. DNA concentration was measured using a NanoDrop spectrophotometer (NanoDrop 2000; Thermo Fisher Scientific, MA, USA).

Genotyping by rep-PCR. rep-PCR was performed as described by Versalovic et al., using primers REP 1R-IDt and REP 2-IDt (REP_1R-IDt, 5′-NNNNCGNCGNCATCNGGC-3′, and REP_2-IDt, 5′-NCGNCT TATCNGGCCTAC-3′) (45). Briefly, the PCR was performed in a total volume of 25 μL containing 5× GoTaq buffer (Promega, Madison, WI, USA), 2.5 mM $MgCl_2$, a 6.25 mM concentration of each deoxynucleoside triphosphate (dNTP), a 50 pM concentration of each primer, 2U of GoTaq DNA polymerase (Promega, Madison, WI, USA) and 100 ng of DNA template. The cycling conditions included initial denaturation at 95°C for 7 min, annealing at 42°C for 60 s, and *Taq* polymerase activation at 65°C for 8 min, followed by 33 cycles of denaturation, annealing, and extension at 94°C for 60 s, 42°C for 30 s, and 65°C for 8 min, respectively, with a final extension at 65°C for 8 min. The reaction was conducted in an Eppendorf Mastercycler Pro thermal cycler (AG 22331; Eppendorf, Hamburg, Germany). The PCR products were run on a 2% TAE buffer (40 mM Tris, 20 mM acetate, and 1 mM EDTA, pH 8.5) agarose gel containing 0.05 μg/mL of ethidium bromide (Sigma-Aldrich, St. Louis, MO, USA) for 3.5 h at 70 V.

The rep-PCR profiles of 44 isolates (from 2020) were compared using BioNumerics software (version 4.50; Applied Maths, Inc., Saint-Martens-Latem, Belgium). Genotypic profiles were compared using band matching tolerance and optimization of 0.5%. For cluster analysis of DNA fingerprinting data, the similarities were calculated using the Dice similarity coefficient (46). A comparison dendrogram was also developed using the unpaired group method with arithmetic average (UPGMA). The genotyping of 19 isolates from 2021 was compared with that of 21 isolates (one representative isolate from each cluster) collected in 2020, using BioNumerics software with the same band matching tolerance and optimization of 0.5%.

Selection of isolates for sequencing. The 44 *Staphylococcus* isolates from 2020 were grouped into 21 clusters using a cutoff threshold of 90% similarity in rep-PCR-based genotyping. A total of 21 isolates were selected (one representative from each cluster) for whole-genome sequencing using the Illumina NovaSeq 6000 (Illumina, San Diego, CA, USA) platform. The selected isolates included three isolates from BFs, two isolates from normal cattle skin, and 16 isolates from BF lesions. Nine of the 21 isolates sequenced with the Illumina platform, including eight isolates from lesions and one from BFs, were also sequenced using the Oxford Nanopore Technologies (ONT) platform to generate complete genomes. These nine isolates were selected at a cutoff threshold of 70% similarity of the genotypic patterns.

DNA extraction and quality testing for sequencing. Selected bacterial isolates were subcultured from storage (−80°C) by inoculation onto 5% (vol/vol) sheep blood agar. The cultures were incubated for 24 h at 37°C. For genome sequencing, DNA was extracted using Gentra Puregene core kit A (Qiagen Pty Ltd., Hilden, Germany) with some modifications of the manufacturer's protocol. A standard suspension from the blood agar (optical density at 600 nm [OD_{600}] = 1.85, or 1.74 × 10^9 bacteria) was prepared in sterile phosphate buffer saline (PBS), and an aliquot of 300 μL was transferred to a 2-mL tube. For efficient lysis, 50 μL of lysozyme (Sigma-Aldrich, St. Louis, MO, USA) at a final concentration of 2.9 mg/mL and 50 μL of lysostaphin at a final concentration of 0.14 mg/mL (Sigma-Aldrich, St. Louis, MO, USA) were also added to each tube and incubated at 37°C for 3 h in a Thermomixer C (Eppendorf, Hamburg, Germany). After 3 h of incubation, 500 μL of cell lysis solution was added to each tube and incubated for 1 h at 56°C. To maximize the DNA yields, the tubes were incubated for 5 min at 80°C. The remaining protocol was followed as recommended by the manufacturer. DNA for sequencing was quantified with a Qubit 4 fluorometer (Thermo Scientific, Waltham, MA, USA) using a Qubit double-stranded-DNA (dsDNA) BR assay kit (Invitrogen, Waltham, MA, USA).

Before library preparation, DNA quality was tested by Pippin pulsed-field gel electrophoresis. For this, 500 ng of the extracted DNA samples was run on a 0.75% SeaKem Gold agarose gel (Lonza Bioscience, Basel, Switzerland) for 16 h on a Pippin Pulse electrophoresis power supply system (Sage

Science, Beverly, MA, USA) at waveform type 5, 430 kb at 80 V. The gel was stained with a 1× concentration of SYBR Safe DNA gel stain (Invitrogen, Waltham, MA, USA).

Illumina library preparation and sequencing. DNA extracted from 21 isolates were sequenced at the Australian Centre for Ecogenomics (ACE), The University of Queensland (St. Lucia, Queensland, Australia). Briefly, DNA libraries were prepared according to the manufacturer's protocol using the Nextera DNA Flex library preparation kit (Illumina, San Diego, CA, USA). Library preparation and bead cleanup were undertaken with the Mantis liquid handler (Formulatrix, Bedford, MA, USA) and Epmotion (Eppendorf, Hamburg, Germany) automated platform. These programs cover "Tagment Genomic DNA" to "Amplify DNA" in the protocol (Nextera DNA Flex library prep protocol; Illumina, San Diego, CA, USA) and "Clean Up Libraries" in the protocol (Epmotion-library cleanup protocol). On completion, each library was quantified, and quality control performed using the Quant-iT dsDNA HS assay kit (Invitrogen, Waltham, MA, USA) and Agilent D1000 HS tapes (Agilent Technologies, Santa Clara, CA, USA) on the TapeStation 4200 (Agilent Technologies, Santa Clara, CA, USA), as per the manufacturer's protocol.

Nextera DNA Flex libraries were pooled at equimolar amounts of 2 nM per library to create a sequencing pool. The library pool was quantified in triplicate using the Qubit dsDNA HS assay kit (Invitrogen, Waltham, MA, USA). Library quality control was performed using the Agilent D1000 HS tapes on the TapeStation 4200 as per the manufacturer's protocol. The library was prepared for sequencing on the NovaSeq 6000 (Illumina, San Diego, CA, USA) using NovaSeq 6000 SP kit v1.5 and 2 × 150-bp paired-end chemistry, according to the manufacturer's protocol.

ONT library preparation. For ONT sequencing, a MinION sequencing library was prepared using the Nanopore Ligation Sequencing kit (Oxford Nanopore Technologies, Oxford, UK) as per the manufacturer's protocol with starting DNA amount of 6 μg (185 fmol). A final amount of 650 ng (20 fmol) of the prepared library was loaded on a MinION Spot-On flow cell (Oxford Nanopore Technologies; version FLO-MIN106D R9.4.1) using a flow cell priming kit (Oxford Nanopore Technologies) as instructed by the manufacturer. The library was sequenced using a MinION device (Mk1C, MC110367) for 5 to 6 h with default instrument settings. Primary acquisition of data and real-time base calling was carried out using the graphical user interface MinKNOW (version 20.10.6; Oxford Nanopore Technologies) and Guppy base caller (v4.5.2; Oxford Nanopore Technologies).

Sequence analysis, assembly, and annotation. All data analysis in this study was performed using programs on Galaxy Australia (https://usegalaxy.org.au/). For each isolate sequenced with the Illumina 6000 NovaSeq platform, 1.0 Gbp of data (400× coverage) was acquired in FASTQ format. Initial read quality was determined by FastQC (Galaxy version, 0.72 + Galaxy1) (http://www.bioinformatics.babraham.ac.uk/projects/fastqc). Low-quality reads were removed using Trimmomatic (Galaxy version 0.36.6) (47) and trimmed from the start (leading) and at the end (trailing) of the reads if the quality score fell below 30. A sliding-window trimming was done if the average quality of four bases dropped below 20, and all unpaired reads and reads below 30 bp were removed. Paired reads were *de novo* assembled using the Shovil assembler (Galaxy version 1.1.0+galaxy0) (with the settings "Estimated genome size": 2.5 Mbps; "Minimum contig length": 500; "Assembler": SPAdes) (https://github.com/tseemann/shovill).

For the isolates sequenced in duplicate with ONT, 2.0 Gbp data (800× coverage) was acquired in FASTQ format. Reads were concatenated using the tool "Concatenate (cat) tail to head" (version 0.1.0 + Galaxy) (https://github.com/bgruening/galaxytools). Reads were filtered for length and average *Q* score by FiltLong (Galaxy version 0.20 + galaxy1) (https://github.com/rrwick/Filtlong). Reads shorter than 5,000 to 15,000 were removed, depending upon the initial read length N_{50} histogram (base-called bases) report generated by Mk1C for an individual isolate. For removal of low-quality reads, a threshold of a *Q* score of ≥7 (for 100% reads) and a *Q* score of ≥12 (for more than 80% reads) was used. The filtered ONT reads along with respective corrected Illumina reads of the same isolate were used to generate hybrid *de novo* assemblies with Unicycler (Galaxy version 0.4.8.0) with normal "Bridging mode" and "Pilon" option enabled for assembly polishing (48). The *de novo* assembled genome sequences were annotated with the prokaryotic genome annotation tool Prokka (Galaxy version 1.14.6+galaxy0) (49).

Pangenome analysis, read mapping, and multilocus sequence phylogeny. To identify the extent of genomic diversity in the sequenced isolates, a pangenome analysis was performed using Roary (Galaxy version 3.13.0+galaxy1) (50). Output from Roary was uploaded on an online web-based platform for interactive visualization of genome phylogenies, Phandango (51), to visualize the presence and absence of a gene and genomic similarity between isolates.

To confirm the identification of the sequenced isolates, corrected paired Illumina reads from all the sequenced isolates were mapped against genomes of reference strains of *S. agnetis* (DSM23656), *S. hyicus* (NCTC10350), *S. chromogenes* (NCTC10530), and *M. sciuri* (NCTC12103) using Bowtie2 (Galaxy version 2.4.2+galaxy0) (52). Accession numbers and the strain type for the genome sequences used for reads mapping are listed in Table 3.

A multilocus sequence phylogeny was constructed using nucleotide sequences of four housekeeping genes (*tuf*, *rpoA*, *rpoB*, and *recN*) from all the annotated genomes from this study and each of the reference strains of *S. agnetis*, *S. hyicus*, *S. chromogenes*, *M. sciuri*, *S. aureus*, *S. caprae*, *S. epidermidis*, *S. intermedius*, *S. argenteus*, and *Bacillus subtilis*. The nucleotide sequences for these four housekeeping genes were concatenated (in the order *tuf*, *rpoA*, *rpoB*, *recN*) and aligned for each genome using Geneious software (version 2021.1.1; Biomatters, Ltd., Auckland, New Zealand). Accession numbers and the strain types for the genome sequences used for phylogenetic analysis are listed in Table 3.

Before phylogenetic analysis, a model test was performed in Mega X (53) with the aligned nucleotide sequences of the above-mentioned genes to select the best suitable model for phylogeny. The model with the lowest Bayesian information criterion (BIC) scores was selected for further analysis. A phylogenetic tree based on concatenated sequences of *tuf*, *rpoA*, *rpoB*, and *recN* was inferred using the

TABLE 3 Bacterial sequences and accession numbers used in genome mapping and phylogenetic analysis

Species	Strain	Accession no.
Staphylococcus agnetis	DSM23656	PPQF01000001
Staphylococcus agnetis	1379	CP045927
Staphylococcus hyicus	NCTC10350	LS483304
Staphylococcus chromogenes	NCTC10530	UHDB01000002
Mammaliicoccus sciuri	NCTC12103	LS483305
Staphylococcus aureus	ATCC 25923	CP009361
Staphylococcus argenteus	DSM28299	JADAMU010000003
Staphylococcus caprae	NCTC12196	UHCW01000006
Staphylococcus epidermidis	ATCC 14990	CP035288
Staphylococcus intermedius	NCTC11048	UHDP01000003
Bacillus subtilis	NCIB3610	CP020102

maximum-likelihood method and general time-reversible model (54) using Mega X (53). Initial trees for the heuristic search were obtained automatically by applying the neighbor-joining and BioNJ algorithms to a matrix of pairwise distances estimated using the maximum-composite-likelihood (MCL) approach. The topology with the superior log likelihood value was then selected. A bootstrap consensus tree inferred from 1,000 replicates was taken to represent the evolutionary history of the taxa analyzed (55). Branches corresponding to partitions reproduced in less than 70% of bootstrap replicates were collapsed. This analysis involved 32 nucleotide sequences. All positions containing gaps and missing data were eliminated (complete deletion option). There was a total of 7,359 nucleotide positions in the final data set.

VF identification. To determine how the isolated bacteria contribute to the development of skin lesions, a comprehensive VF search was undertaken to identify potential VF resembling previously reported VF among staphylococcal and nonstaphylococcal species, including those previously shown to cause skin infections.

To identify the VF sequences, present in each bacterial isolate, a comprehensive VF data set of staphylococci (CVFS) developed by Naushad et al. (31) was used. Briefly, this custom database was created from the amino acid sequences of the VF for the genus *Staphylococcus* obtained from publicly available databases, including the Victor database (https://doi.org/10.1093/nar/gky999), the PATRIC database (56), and the VFDB database (57), and phenol-soluble-modulin sequences from the UniProtKB database (58). Cutoffs of ≥30% amino acid sequence similarity, ≥50% query length coverage, and bit score of ≥100 were used to confirm VF presence or absence in the genomes of the corresponding isolates (59–61).

For robust identification of VF and to identify any VF resembling non-*Staphylococcus* species in our isolates, we assigned identity based on cutoffs of ≥50% amino acid sequence similarity, ≥50% query length coverage, and bit score of ≥100, with the amino acid sequences of VFCD from VFDB (57). This was conducted using custom BLAST databases for CVFS and VFCD formatted using "NCBI BLAST + makeblastdb" (Galaxy version 2.10.1+galaxy0) (62–64) and homology of all amino acids identified in the annotated genomes determined using "NCBI BLAST + BLASTp" (Galaxy version 2.10.1+galaxy0) (62–64). As two databases were used for the designation of gene names, to prevent any duplication of gene annotation, the amino acid query sequence with the highest similarity score obtained was used for further analysis.

Exfoliative toxin analysis. The relationships between the exfoliative toxins identified from isolates in this study and other publicly available amino acid sequences for exfoliative toxins A (*eta*) and C (*etc*) of *Staphylococcus* spp. was determined by amino acid sequence alignment in Geneious (version 2021.1.1; Biomatters Ltd., Auckland, New Zealand) and phylogenetic analysis. For *eta*, amino acid sequences for exfoliative toxin A from *S. hyicus* (accession no. AB036768) and *S. aureus* strains MSSA476, N315, NCTC8325, USA300, MRSA252, and RF122 (VFCD IDs VFG004880, VFG004849, VFG004878, VFG004876, VFG004881, and VFG004877, respectively) were aligned with *eta* sequences from the current study in Geneious (version 2021.1.1; Biomatters Ltd., Auckland, New Zealand). For *etc*, amino acid sequences from *S. aureus* (accession no. BAA99412), *M. sciuri* (accession no. JF755400), and *S. hyicus* (accession no. AF515455 and KT072730) were aligned with *etc* sequences identified from this study using the same software.

To select the best suitable model for phylogenetic analysis of *eta* and *etc* genes, a model test was performed in Mega X (53) with amino acid sequences from both genes, and the model with the lowest BIC scores was chosen for further analysis. Phylogenetic trees were inferred for *eta* and *etc*, respectively, using the maximum-likelihood method and general reversible chloroplast model (65) in Mega X. Initial trees for the heuristic search were obtained automatically by applying the neighbor-joining and BioNJ algorithms to a matrix of pairwise distances estimated using the JTT model. The topology with a superior log likelihood value was then selected. The bootstrap consensus tree inferred from 1,000 replicates was taken to represent the evolutionary history of the taxa analyzed (55). Branches corresponding to partitions reproduced in less than 70% of the bootstrap replicates were collapsed. For the *eta* and *etc* proteins, 27 and 25 amino acid sequences and 306 and 280 amino acid positions were involved, respectively.

PCR based identification of isolates. To identify the isolates from 2021 sampling and to confirm the identity of isolates from 2020 which were not utilized for genome sequencing, DNA samples extracted from each of the isolates were tested with an *aroD*-based multiplex PCR using the primers

reported by Adkins et al. for species-specific identification of *S. hyicus* (aroD_hyF, 5′-TATGGTG TCGACCAATCGAAGGCT-3′, and aroD_hyR, 5′-ACCCTATAGCCCGCTTAC-TT-3′) and *S. agnetis* (aroD_agF, 5′-CGCATGAGAGACCAATACGCT-3′, and aroD_agR, 5′-TAGGACGTATAGAGGTGG-3′) (22). Briefly, the PCR was performed in a total volume of 20 μL containing 10 μL of 2× Phusion Hot Start II high-fidelity PCR master mix (Thermo Scientific, Waltham, MA, USA), a 10 μM concentration of each forward and reverse primer, and 3 ng of DNA template. The cycling conditions included an initial denaturation at 98°C for 30 s, followed by 30 cycles of denaturation, annealing, and extension at 98°C for 10 s, 60°C for 30 s, and 72°C for 30 s, respectively, and a final extension at 72°C for 10 m. The reaction was set up in an Eppendorf Mastercycler Pro thermal cycler. For visualization, the amplification products were run on 2% TBE buffer (89 mM Tris, 89 mM boric acid, and 2 mM EDTA, pH 8) agarose gel for 75 m at 80 V using a GeneRuler 100-bp Plus DNA ladder (Thermo Fisher Scientific, Waltham, MA, USA).

Data availability. The sequence data generated and analyzed in the current study have been deposited in the NCBI genome database (https://www.ncbi.nlm.nih.gov/genome) under BioProject accession number PRJNA809943.

ACKNOWLEDGMENTS

The authors thank the Meat and Livestock Australia (MLA) Donor Company, Grant P.PSH.0798, for funding this research. We are also grateful to the University of Queensland Pinjarra Hills Research Precinct staff (Alison Moore and Tom Connelly) for their help in sample collection.

REFERENCES

1. Hibler CP. 1966. Development of *Stephanofilaria stilesi* in the horn fly. J Parasitol 52:890–898. https://doi.org/10.2307/3276527.
2. Johnson SJ. 1989. Studies of stephanofilariasis in Queensland. PhD Thesis. James Cook University, Douglas, Australia.
3. Jonsson NN, Mayer DG. 1999. Estimation of the effects of buffalo fly (*Haematobia irritans exigua*) on the milk production of dairy cattle based on a meta-analysis of literature data. Med Vet Entomol 13:372–376. https://doi.org/10.1046/j.1365-2915.1999.00179.x.
4. James P, Madhav M, Brown G. 2020. Buffalo flies (*Haematobia exigua*) expanding their range in Australia, p 463–482. *In* Hendrichs J, Pereira R, Vreysen MJB (ed). Area-wide integrated pest management: development and field application, vol 1. CRC Press, Boca Raton, FL, USA.
5. Johnson SJ, Parker RJ, Norton JH, Jaques PA, Grimshaw AA. 1981. Stephanofilariasis in cattle. Aust Vet J 57:411–413. https://doi.org/10.1111/j.1751-0813.1981.tb00544.x.
6. Sutherst RW, Bourne AS, Maywald GF, Seifert GW. 2006. Prevalence, severity, and heritability of *Stephanofilaria* lesions on cattle in central and southern Queensland, Australia. Aust J Agric Res 57:743–750. https://doi.org/10.1071/AR05265.
7. Johnson SJ, Arthur RJ, Shepherd RK. 1986. The distribution and prevalence of stephanofilariasis in cattle in Queensland. Aust Vet J 63:121–124. https://doi.org/10.1111/j.1751-0813.1986.tb07679.x.
8. Naseem MN, Raza A, Fordyce G, McGowan M, Constantinoiu C, Turni C, Allavena R, Tabor AE, James P. 2022. Detection and distribution of Stephanofilaria sp. in buffalo fly lesions and buffalo flies in north Australian beef cattle. Vet Parasitol 305. https://doi.org/10.1016/j.vetpar.2022.109715.
9. Edwards JF, Wikse SE, Field RW, Hoelscher CC, Herd DB. 2000. Bovine teat atresia associated with horn fly (*Haematobia irritans irritans* (L.))-induced dermatitis. Vet Pathol 37:360–364. https://doi.org/10.1354/vp.37-4-360.
10. Owens WE, Oliver SP, Gillespie BE, Ray CH, Nickerson SC. 1998. Role of horn flies (*Haematobia irritans*) in *Staphylococcus aureus*-induced mastitis in dairy heifers. Am J Vet Res 59:1122–1124.
11. Nickerson SC, Owens WE, Boddie RL. 1995. Mastitis in dairy heifers: initial studies on prevalence and control. J Dairy Sci 78:1607–1618. https://doi.org/10.3168/jds.S0022-0302(95)76785-6.
12. Gillespie BE, Owens WE, Nickerson SC, Oliver SP. 1999. Deoxyribonucleic acid fingerprinting of *Staphylococcus aureus* from heifer mammary secretions and from horn flies. J Dairy Sci 82:1581–1585. https://doi.org/10.3168/jds.S0022-0302(99)75386-5.
13. Palavesam A, Guerrero FD, Heekin AM, Wang J, Dowd SE, Sun Y, Foil LD, Pérez-de-León AA. 2012. Pyrosequencing-based analysis of the microbiome associated with the horn fly, *Haematobia irritans*. PLoS One 7:e44390. https://doi.org/10.1371/journal.pone.0044390.
14. Devriese LA, Derycke J. 1979. *Staphylococcus hyicus* in cattle. Res Vet Sci 26:356–358. https://doi.org/10.1016/S0034-5288(18)32893-5.
15. Hazarika RA, Mahanta PN, Dutta GN, Devriese LA. 1991. Cutaneous infection associated with *Staphylococcus hyicus* in cattle. Res Vet Sci 50:374–375. https://doi.org/10.1016/0034-5288(91)90146-f.
16. Devriese LA, Vlaminck K, Nuytten J, Keersmaecker P. 1983. *Staphylococcus hyicus* in skin lesions of horses. Equine Vet J 15:263–265. https://doi.org/10.1111/j.2042-3306.1983.tb01786.x.
17. Hassler C, Nitzsche S, Iversen C, Zweifel C, Stephan R. 2008. Characteristics of *Staphylococcus hyicus* strains isolated from pig carcasses in two different slaughterhouses. Meat Sci 80:505–510. https://doi.org/10.1016/j.meatsci.2008.02.001.
18. Schamber G, Alstad AD. 1989. Isolation of *Staphylococcus hyicus* from seborrheic dermatitis in a pygmy goat. J Vet Diagn Invest 1:276–277. https://doi.org/10.1177/104063878900100320.
19. Wegener HC, Andresen LO, Bille-Hansen V. 1993. *Staphylococcus hyicus* virulence in relation to exudative epidermitis in pigs. Can J Vet Res 57:119–125.
20. Ahrens P, Andresen LO. 2004. Cloning and sequence analysis of genes encoding *Staphylococcus hyicus* exfoliative toxin types A, B, C, and D. J Bacteriol 186:1833–1837. https://doi.org/10.1128/JB.186.6.1833-1837.2004.
21. Sato H, Watanabe T, Higuchi K, Teruya K, Ohtake A, Murata Y, Saito H, Aizawa C, Danbara H, Maehara N. 2000. Chromosomal and extrachromosomal synthesis of exfoliative toxin from *Staphylococcus hyicus*. J Bacteriol 182:4096–4100. https://doi.org/10.1128/JB.182.14.4096-4100.2000.
22. Adkins PRF, Middleton JR, Calcutt MJ, Stewart GC, Fox LK. 2017. Species identification and strain typing of *Staphylococcus agnetis* and *Staphylococcus hyicus* isolates from bovine milk by use of a novel multiplex PCR assay and pulsed-field gel electrophoresis. J Clin Microbiol 55:1778–1788. https://doi.org/10.1128/JCM.02239-16.
23. Roberson JR, Fox LK, Hancock DD, Gay JM, Besser TE. 1996. Prevalence of coagulase-positive staphylococci other than *Staphylococcus aureus* in bovine mastitis. Am J Vet Res 57:54–58.
24. Al-Rubaye AA, Couger MB, Ojha S, Pummill JF, Koon JA, Wideman RF, Jr, Rhoads DD. 2015. Genome analysis of *Staphylococcus agnetis*, an agent of lameness in broiler chickens. PLoS One 10:e0143336. https://doi.org/10.1371/journal.pone.0143336.
25. Taponen S, Supré K, Piessens V, Van Coillie E, De Vliegher S, Koort JMK. 2012. *Staphylococcus agnetis* sp. nov., a coagulase-variable species from bovine subclinical and mild clinical mastitis. Int J Syst Evol Microbiol 62:61–65. https://doi.org/10.1099/ijs.0.028365-0.
26. Anderson KL, Lyman R, Moury K, Ray D, Watson DW, Correa MT. 2012. Molecular epidemiology of *Staphylococcus aureus* mastitis in dairy heifers. J Dairy Sci 95:4921–4930. https://doi.org/10.3168/jds.2011-4913.
27. Pizauro LJL, de-Almeida CC, Soltes GA, Slavic D, Rossi-Junior OD, de-Ávila FA, Zafalon LF, MacInnes JI. 2017. Species level identification of coagulase negative *Staphylococcus* spp. from buffalo using matrix-assisted laser desorption ionization–time of flight mass spectrometry and cydB real-time quantitative PCR. Vet Microbiol 204:8–14. https://doi.org/10.1016/j.vetmic.2017.03.036.
28. Wanecka A, Król J, Twardoń J, Mrowiec J, Korzeniowska-Kowal A, Wzorek A. 2019. Efficacy of MALDI-TOF mass spectrometry as well as genotypic and phenotypic methods in identification of staphylococci other than *Staphylococcus aureus* isolated from intramammary infections in dairy

cows in Poland. J Vet Diagn Invest 31:523–530. https://doi.org/10.1177/1040638719845423.
29. Jousson O, Di-Bello D, Vanni M, Cardini G, Soldani G, Pretti C, Intorre L. 2007. Genotypic versus phenotypic identification of staphylococcal species of canine origin with special reference to *Staphylococcus schleiferi* subsp. coagulans. Vet Microbiol 123:238–244. https://doi.org/10.1016/j.vetmic.2007.02.020.
30. Adkins PRF, Dufour S, Spain JN, Calcutt MJ, Reilly TJ, Stewart GC, Middleton JR. 2018. Cross-sectional study to identify staphylococcal species isolated from teat and inguinal skin of different-aged dairy heifers. J Dairy Sci 101:3213–3225. https://doi.org/10.3168/jds.2017-13974.
31. Naushad S, Naqvi SA, Nobrega D, Luby C, Kastelic JP, Barkema HW, De Buck J. 2019. Comprehensive virulence gene profiling of bovine non-aureus staphylococci based on whole-genome sequencing data. mSystems 4:e00098-18. https://doi.org/10.1128/mSystems.00098-18.
32. Tremblay YD, Lamarche D, Chever P, Haine D, Messier S, Jacques M. 2013. Characterization of the ability of coagulase-negative staphylococci isolated from the milk of Canadian farms to form biofilms. J Dairy Sci 96:234–246. https://doi.org/10.3168/jds.2012-5795.
33. Arnosti C. 2011. Microbial extracellular enzymes and the marine carbon cycle. Annu Rev Mar Sci 3:401–425. https://doi.org/10.1146/annurev-marine-120709-142731.
34. Åvall-Jääskeläinen S, Taponen S, Kant R, Paulin L, Blom J, Palva A, Koort J. 2018. Comparative genome analysis of 24 bovine-associated *Staphylococcus* isolates with special focus on the putative virulence genes. PeerJ 6:e4560. https://doi.org/10.7717/peerj.4560.
35. Kuipers A, Stapels DAC, Weerwind LT, Ko YP, Ruyken M, Lee JC, van-Kessel KPM, Rooijakkers SHM. 2016. The *Staphylococcus aureus* polysaccharide capsule and Efb-dependent fibrinogen shield act in concert to protect against phagocytosis. Microbiology (Reading)source> 162:1185–1194. https://doi.org/10.1099/mic.0.000293.
36. Marques VF, Souza M, de-Mendonça EC, Alencar TAd, Pribul BR, Coelho SMO, Lasagno M, Reinoso EB. 2013. Phenotypic and genotypic analysis of virulence in *Staphylococcus* spp. and its clonal dispersion as a contribution to the study of bovine mastitis. Pesq Vet Bras 33:161–170. https://doi.org/10.1590/S0100-736X2013000200005.
37. Haley KP, Skaar EP. 2012. A battle for iron: host sequestration and *Staphylococcus aureus* acquisition. Microbes Infect 14:217–227. https://doi.org/10.1016/j.micinf.2011.11.001.
38. Hammer ND, Skaar EP. 2011. Molecular mechanisms of *Staphylococcus aureus* iron acquisition. Annu Rev Microbiol 65:129–147. https://doi.org/10.1146/annurev-micro-090110-102851.
39. Sheldon JR, Heinrichs DE. 2015. Recent developments in understanding the iron acquisition strategies of gram positive pathogens. FEMS Microbiol Rev 39:592–630. https://doi.org/10.1093/femsre/fuv009.
40. Ates LS, Houben EN, Bitter W. 2016. Type VII secretion: a highly versatile secretion system. Microbiol Spectr 4:VMBF-0011-2015. https://doi.org/10.1128/microbiolspec.VMBF-0011-2015.
41. Warne B, Harkins CP, Harris SR, Vatsiou A, Stanley-Wall N, Parkhill J, Peacock SJ, Palmer T, Holden MT. 2016. The Ess/type VII secretion system of *Staphylococcus aureus* shows unexpected genetic diversity. BMC Genom 17:222. https://doi.org/10.1186/s12864-016-2426-7.
42. Fudaba Y, Nishifuji K, Andresen LO, Yamaguchi T, Komatsuzawa H, Amagai M, Sugai M. 2005. *Staphylococcus hyicus* exfoliative toxins selectively digest porcine desmoglein 1. Microb Pathog 39:171–176. https://doi.org/10.1016/j.micpath.2005.08.003.
43. Nayduch D, Cho H, Joyner C. 2013. *Staphylococcus aureus* in the house fly: temporospatial fate of bacteria and expression of the antimicrobial peptide defensin. J Med Entomol 50:171–178. https://doi.org/10.1603/me12189.
44. Halebian S, Harris B, Finegold SM, Rolfe RD. 1981. Rapid method that aids in distinguishing Gram-positive from Gram-negative anaerobic bacteria. J Clin Microbiol 13:444–448. https://doi.org/10.1128/jcm.13.3.444-448.1981.
45. Versalovic J, Koeuth T, Lupski JR. 1991. Distribution of repetitive DNA sequences in eubacteria and application to fingerprinting of bacterial genomes. Nucleic Acids Res 19:6823–6831. https://doi.org/10.1093/nar/19.24.6823.
46. Dice LR. 1945. Measures of the amount of ecologic association between species. Ecology 26:297–302. https://doi.org/10.2307/1932409.
47. Bolger AM, Lohse M, Usadel B. 2014. Trimmomatic: a flexible trimmer for Illumina sequence data. Bioinformatics 30:2114–2120. https://doi.org/10.1093/bioinformatics/btu170.
48. Wick RR, Judd LM, Gorrie CL, Holt KE. 2017. Unicycler: resolving bacterial genome assemblies from short and long sequencing reads. PLoS Comput Biol 13:e1005595. https://doi.org/10.1371/journal.pcbi.1005595.
49. Cuccuru G, Orsini M, Pinna A, Sbardellati A, Soranzo N, Travaglione A, Uva P, Zanetti G, Fotia G. 2014. Orione, a web-based framework for NGS analysis in microbiology. Bioinformatics 30:1928–1929. https://doi.org/10.1093/bioinformatics/btu135.
50. Page A, Cummins CA, Hunt M, Wong VK, Reuter S, Holden MT, Fookes M, Falush D, Keane JA, Parkhill J. 2015. Roary: rapid large-scale prokaryote pan genome analysis. Bioinformatics 31:3691–3693. https://doi.org/10.1093/bioinformatics/btv421.
51. Hadfield J, Croucher NJ, Goater RJ, Abudahab K, Aanensen DM, Harris SR. 2018. Phandango: an interactive viewer for bacterial population genomics. Bioinformatics 34:292–293. https://doi.org/10.1093/bioinformatics/btx610.
52. Langmead B, Trapnell C, Pop M, Salzberg SL. 2009. Ultrafast and memory-efficient alignment of short DNA sequences to the human genome. Genome Biol 10:R25. https://doi.org/10.1186/gb-2009-10-3-r25.
53. Kumar S, Stecher G, Li M, Knyaz C, Tamura K. 2018. MEGA X: molecular evolutionary genetics analysis across computing platforms. Mol Biol Evol 35:1547–1549. https://doi.org/10.1093/molbev/msy096.
54. Nei M, Kumar S. 2000. Molecular evolution and phylogenetics. Oxford University Press, New York, NY, USA.
55. Felsenstein J. 1985. Confidence limits on phylogenies: an approach using the bootstrap. Evol 39:83–791.
56. Wattam AR, Abraham D, Dalay O, Disz TL, Driscoll T, Gabbard JL, Gillespie JJ, Gough R, Hix D, Kenyon R, Machi D, Mao C, Nordberg EK, Olson R, Overbeek R, Pusch GD, Shukla M, Schulman J, Stevens RL, Sullivan DE, Vonstein V, Warren A, Will R, Wilson MJC, Yoo HS, Zhang C, Zhang Y, Sobral BW. 2014. PATRIC, the bacterial bioinformatics database and analysis resource. Nucleic Acids Res 42:D581–D591. https://doi.org/10.1093/nar/gkt1099.
57. Chen L, Zheng D, Liu B, Yang J, Jin Q. 2016. VFDB 2016: hierarchical and refined dataset for big data analysis—10 years on. Nucleic Acids Res 44:D694–D697. https://doi.org/10.1093/nar/gkv1239.
58. The UniProt Consortium. 2017. UniProt: the universal protein knowledgebase. Nucleic Acids Res 45:D158–D169. https://doi.org/10.1093/nar/gkw1099.
59. Pearson WR. 2013. An introduction to sequence similarity ("homology") searching. Curr Protoc Bioinformatics Chapter 3:Unit 3.1. https://doi.org/10.1002/0471250953.bi0301s42.
60. Pearson WR. 2013. Selecting the right similarity-scoring matrix. Curr Protoc Bioinformatics 43:3.5.1–3.5.9. https://doi.org/10.1002/0471250953.bi0305s43.
61. Rost B. 1999. Twilight zone of protein sequence alignments. Protein Eng 12:85–94. https://doi.org/10.1093/protein/12.2.85.
62. Altschul SF, Madden TL, Schäffer AA, Zhang J, Zhang Z, Miller W, Lipman DJ. 1997. Gapped BLAST and PSI-BLAST: a new generation of protein database search programs. Nucleic Acids Res 25:3389–3402. https://doi.org/10.1093/nar/25.17.3389.
63. Camacho C, Coulouris G, Avagyan V, Ma N, Papadopoulos J, Bealer K, Madden TL. 2009. BLAST+: architecture and applications. BMC Bioinform 10:421. https://doi.org/10.1186/1471-2105-10-421.
64. Cock PJA, Chilton JM, Grüning B, Johnson JE, Soranzo N. 2015. NCBI BLAST+ integrated into Galaxy. GigaScience 4:39. https://doi.org/10.1186/s13742-015-0080-7.
65. Adachi J, Waddell PJ, Martin W, Hasegawa M. 2000. Plastid genome phylogeny and a model of amino acid substitution for proteins encoded by chloroplast DNA. J Mol Evol 50:348–358. https://doi.org/10.1007/s002399910038.